

1 **Pliocene–Early Pleistocene climatic trends in the Italian Peninsula based on stable**
2 **oxygen and carbon isotope compositions of rhinoceros and gomphothere tooth enamel**

3

4 Péter Szabó^{a,b,c,*}, László Kocsis^d, Torsten Vennemann^c, Luca Pandolfi^c, János Kovács^{a,f},
5 Edoardo Martinetto^g, Attila Demény^h

6

7 ^a *Environmental Analytical and Geoanalytical Research Group, Szentágotthai Research*
8 *Centre, University of Pécs, Pécs, Hungary*

9 ^b *Doctoral School of Chemistry, University of Pécs, Pécs, Hungary*

10 ^c *Faculty of Geosciences and Environment, Géopolis, Institute of Earth Surface Dynamics,*
11 *University of Lausanne, Lausanne, Switzerland*

12 ^d *Geology Group, Faculty of Science, Universiti Brunei Darussalam - UBD, Brunei*
13 *Darussalam*

14 ^e *Department of Sciences, section of Geology. University of Roma TRE, Roma, Italy*

15 ^f *Department of Geology and Meteorology. University of Pécs, Pécs, Hungary*

16 ^g *Department of Earth Sciences, University of Torino, Torino, Italy*

17 ^h *Institute of Geological and Geochemical Research Research Centre for Astronomy and*
18 *Earth Sciences, Budapest, Hungary,*

19

20 *E-mail address of corresponding author: sz.piiit01@gmail.com

21

22

23 **Abstract**

24

25 The Pliocene and Early Pleistocene (5.2 to 1 Ma) palaeoclimate for localities in Italy is
26 evaluated using stable carbon and oxygen isotope compositions of tooth enamel of fossil
27 specimens from Rhinocerotidae (*Stephanorhinus* sp.) and Gomphotheriidae (*Anancus* sp.)
28 taxa. Carbon isotope composition was measured in the structural carbonate ($\delta^{13}\text{C}$), while
29 oxygen isotope values were determined both in the structural carbonate ($\delta^{18}\text{O}_{\text{CO}_3}$) and the
30 phosphate ($\delta^{18}\text{O}_{\text{PO}_4}$) of bioapatite.

31 The $\delta^{13}\text{C}_{\text{CO}_3}$ values indicate that the taxa were grazers-browsers of a pure C_3 vegetation. Low
32 $\delta^{13}\text{C}_{\text{CO}_3}$ values for Central and North Italy indicate a humid climate with woodlands and forest
33 cover in the Pliocene. For northern localities the $\delta^{13}\text{C}$ values increase between MN16a and
34 MNQ16b biozones most likely linked to the Northern Hemisphere Glaciation at 2.7 Ma after
35 the "Mid-Pliocene Warm Period". For Central Italy the values have a wide range with a long
36 term increasing trend in the Early Pleistocene, indicating more arid climate and / or more
37 open vegetation.

38 Overall, the $\delta^{18}\text{O}_{\text{PO}_4}$ values in Central Italy change together with the $\delta^{13}\text{C}_{\text{CO}_3}$ values and are
39 taken to reflect the warmer / wetter interglacials and cooler / more arid glacial phases. The
40 $\delta^{18}\text{O}_{\text{PO}_4}$ values in North Italy are lower than those in Central Italy and show no clear temporal
41 trend. One explanation for the low values especially in MN14-15 biozone is that these $\delta^{18}\text{O}_{\text{PO}_4}$
42 values do not reflect entirely the isotopic composition of local precipitation but river waters
43 from the Alps with ^{18}O -depleted isotopic compositions or a N-S directed rain-shadow effect
44 on the precipitation. In general the new isotope data agree well with palaeoclimate
45 reconstructions based on palynological and other proxies.

46

47 Keywords: stable isotopes, enamel, climate, Pliocene, Early Pleistocene, Italy

48

49 **1. Introduction**

50

51 There is an increasing interest in understanding Pliocene and Early Pleistocene terrestrial
52 climates and environments because it can help to predict future climate changes more
53 accurately. Reconstructions of terrestrial palaeoenvironments, palaeoecology, and
54 palaeoclimates are commonly based on proxies like paleosols, fossil plants (including pollen),
55 vertebrate occurrences, speleothems, travertines, tufas, as well as the geochemistry and
56 isotope geochemistry of biogenic carbonates and phosphates such as mammal teeth and
57 bones. (Sullivan and Krüger, 1983; Luz et al., 1984; 1990; Luz and Kolodny, 1985; Lee-
58 Thorp and van der Merwe, 1987; Lee-Thorp et al., 1989; Ayliffe et al., 1992; 1994; Bryant
59 and Froelich, 1995; Bocherens et al., 1996; Fricke et al., 1998; Cerling and Harris, 1999;
60 Kohn et al., 1999; Kohn and Cerling, 2002; Arppe and Karhu, 2006; Levin et al., 2006;
61 Tütken et al., 2006; Martin et al., 2008; Kohn, 2010; Pellegrini et al., 2011; Kocsis et al.,
62 2014; Pushkina et al., 2014; García-Alix, 2015; Kovács et al., 2015; Hartman et al., 2016;
63 Metcalfe et al., 2016 and references therein).

64 In this study 51 Pliocene and Early Pleistocene tooth enamel samples of fossil rhinoceros ($n =$
65 44) and gomphothere ($n = 7$) were studied from Italy. Most of the samples are from Central
66 and North Italy and a few samples from South Italy (Figure 1). The age of the fossils covers
67 the Early Pliocene to late Early Pleistocene, from about 5.2 to 1 Ma.

68 The carbon and oxygen isotope compositions of structural carbonate and the oxygen isotope
69 composition of phosphate in enamel bioapatite were used to explore variations in past climate
70 and the environment of the animals. The aims of this study are: 1) Reconstructing the isotope
71 composition of environmental water ($\delta^{18}\text{O}_w$) and estimating the changes in mean annual
72 surface air temperature (MAT) on the basis of $\delta^{18}\text{O}_{\text{PO}_4}$ values of fossil tooth enamel; 2)

73 interpretation of the diet of the species; 3) detect changes in vegetation based on the enamel
74 carbon isotope analyses.

75 These climatic and ecological parameters derived from the isotope results are compared with
76 palaeobotanical proxies, palaeontological and palaeoecological information (Fauquette et al.,
77 1999; Pontini and Bertini, 2000; Bertini, 2001; 2010; Bredenkamp et al., 2002; Ji et al., 2002;
78 Fauquette and Bertini, 2003; Klotz et al., 2006; Palombo, 2007; Magri et al., 2010; Rook and
79 Martínez-Navarro, 2010; Petronio et al., 2011; Combourieu-Nebout et al., 2015; Loftus et al.,
80 2015; Rivals et al., 2015).

81

82 **2. Background**

83

84 *2.1. Bioapatite and preservation of its isotopic compositions*

85

86 Biogenic hydroxyapatite (i.e., bioapatite) is the main inorganic fraction of the skeletal tissues
87 of mammals with up to 6 wt.% of carbonate as structurally bound carbonate. The simplified
88 formula is $\text{Ca}_5(\text{PO}_4, \text{CO}_3)_3(\text{OH}, \text{CO}_3)$ (e.g., Kohn et al., 1999; Elliot, 2002). There are two
89 types of carbonate forms in bioapatite, structural and labile carbonate. Structural carbonate
90 substitutes for PO_4^{3-} and OH^- , while the labile CO_3^{2-} component's structural identity is
91 ambiguous as it is often considered adsorbed onto the surface. Oxygen is present in three
92 different ions in bioapatite: phosphate, hydroxyl and carbonate ions. Because of the strong P–
93 O bonds phosphate oxygen is considered more resistant to low temperature inorganic
94 alteration processes, than carbonate oxygen (Kohn et al., 1999; Kohn and Cerling, 2002).
95 However, during microbiological reactions even the phosphate oxygen isotope composition
96 can be changed due to enzymatic catalysis between PO_4^{3-} and water (e.g., Blake et al., 1997;
97 Zazzo, 2004a,b; Liang and Blake, 2007). Nevertheless, it was shown experimentally that

98 when enamel (i.e., well-crystalized bioapatite) is subjected to bacterially mediated conditions,
99 the oxygen isotopic composition of the phosphate group was not affected (e.g., Zazzo,
100 2004a,b). Moreover, enamel is the preferred tissue for isotopic investigations because it
101 contains the highest proportion of apatite (96%), and structurally compact with little pore
102 space and large phosphate crystallites (up to 1 μm long), arranged in a decussate texture
103 (Kohn et al., 1999). As a result enamel is more resistant to diagenesis than other tissues in the
104 same taphonomic context (Lee-Thorp and van der Merwe, 1991; Quade et al., 1992; Ayliffe
105 et al., 1994; Wang and Cerling, 1994; Koch et al., 1997).

106 There is a widely used method to monitor diagenetic effects. Oxygen from the body fluids is
107 in isotopic equilibrium with both the carbonate and phosphate ions of the inorganic tissue.
108 Several studies have found a constant offset between the $\delta^{18}\text{O}_{\text{CO}_3}$ and $\delta^{18}\text{O}_{\text{PO}_4}$ values for non-
109 altered mammal tooth enamel and the $\delta^{18}\text{O}_{\text{CO}_3} - \delta^{18}\text{O}_{\text{PO}_4}$ slopes are similar for different
110 species (Bryant et al., 1996; Iacumin et al., 1996; Arppe and Karhu, 2006, 2010; Tütken et al.,
111 2007; Pellegrini et al., 2011; Domingo et al., 2013). Because it seems quite improbable to find
112 isotopically altered skeletal remains showing a good correlation and a similar offset to
113 modern samples, it is plausible to use the parallel $\delta^{18}\text{O}_{\text{CO}_3} - \delta^{18}\text{O}_{\text{PO}_4}$ measurements as a
114 monitor of diagenetic alteration (Iacumin et al., 1996). Most studies found an offset 8.4 – 9.1
115 ‰ for modern, unaltered samples (Bryant et al., 1996; Iacumin et al., 1996; Martin et al.,
116 2008; Pellegrini et al., 2011). Nevertheless, Martin et al. (2008) found ~ 2 ‰ intra tooth
117 differences in two upper molars (M1 and M2) of extant *Rhinoceros unicornis* and further
118 variations can be present due to environmental, physiological and tooth growth process
119 differences. The final recommendation is that if the $\delta^{18}\text{O}_{\text{CO}_3} - \delta^{18}\text{O}_{\text{PO}_4}$ difference is in the
120 range of 7.2 ‰ to 10.6 ‰ the values of the samples can be considered as unaltered (Martin et
121 al., 2008).

122

123 2.2. *Stable carbon isotope composition and diet*

124

125 Carbon isotope differences among vertebrates largely reflect the differences in the diet of the
126 animals. Variations in $\delta^{13}\text{C}$ values of the plants reflect mostly the three different
127 photosynthetic pathways used by plants. The C_3 pathway is the most common, occurring in all
128 trees, most shrubs and herbs, and grasses in regions with a cool-temperate growing season. C_3
129 plants have a mean $\delta^{13}\text{C}$ value of about -27‰ with a range from -35 to -22‰ . C_4
130 photosynthesis occurs in grasses from regions with a warm growing season, and in some
131 sedges (Bruhl and Wilson, 2007) and dicots. C_4 plants have higher $\delta^{13}\text{C}$ values (mean ca. -13
132 ‰ , range between -19 and -9‰). Crassulacean acid metabolism (CAM) is the least common
133 pathway, occurring mostly in succulent plants, with a range between the C_3 and C_4 plants
134 (O'Leary, 1988; Farquhar et al., 1989; Martinelli et al., 1991). Enamel $\delta^{13}\text{C}$ values of large
135 non-ruminant herbivores have a bioapatite-plant fractionation offset of about 13.3‰ (Passey
136 et al., 2005). In C_3 ecosystems, the variation in $\delta^{13}\text{C}$ values can provide further information
137 about mean annual precipitation (MAP), humidity, the type of vegetation, habitat differences
138 or niche partitioning between animals (Van der Merwe and Medina, 1991; Feranec and
139 MacFadden, 2006; Kohn, 2010). Generally C_3 plants show a monotonic increase in $\delta^{13}\text{C}$ with
140 decreasing MAP (Kohn, 2010). Effects of vegetation like the canopy effect complicate this
141 relationship though. In forests the limited sunlight availability, high relative humidity and the
142 low $\delta^{13}\text{C}_{\text{CO}_2}$ values from decaying litter of the soil organic matter lowers the $\delta^{13}\text{C}$ values (Van
143 der Merwe and Medina, 1991; Bocherens et al., 1996; Cerling and Harris, 1999; Drucker et
144 al., 2008). As the $\delta^{13}\text{C}$ values of herbivores reflect the values of the consumed plants,
145 preferential consumption of some specific plants could imply that the $\delta^{13}\text{C}$ values of apatite
146 can not be taken to determine the average vegetation. Food preference of the animals is also

147 not necessarily constant within a taxonomic group, and for a given taxon through space and
148 time.

149 Because of the complex information encoded in the $\delta^{13}\text{C}$ values, several studies applied it to
150 address a variety of palaeodietary, palaeoecological, and palaeoenvironmental problems (e.g.
151 Lee-Thorp et al., 1989; Quade et al., 1992; Bocherens et al., 1996; Cerling et al., 1999;
152 Iacumin et al., 2000; Feranec, 2004; Metcalfe et al., 2009; Arppe et al., 2011; Montanari et
153 al., 2013; Kocsis et al., 2014; Scherler et al., 2014; Zanazzi et al., 2015).

154

155 *2.3. Stable oxygen isotope composition and environmental water*

156

157 Oxygen isotope compositions of mammal teeth are linearly related to the body water of the
158 animals (Longinelli, 1984). The isotope composition of body water depends on the total
159 oxygen flux through the body, but water from drinking and food sources have the largest
160 effect compared to other factors (Luz, 1984). In the case of elephants the ratio is
161 approximately 2:1 of water ingested via drinking and that ingested by consumption of plant
162 matter (Ayliffe et al., 1992), while for rhinoceroses this ratio is 4:1 (Clauss et al., 2005;
163 Martin et al., 2008). Thus teeth of these two groups are potentially good indicators of the $\delta^{18}\text{O}$
164 values of local environmental waters (Martin et al., 2008). The drinking water of the animals
165 may include different sources including streams, ponds, rivers, lakes, and leaves. Each of
166 these reservoirs typically can have different $\delta^{18}\text{O}$ values relative to precipitation, due to
167 variable mixing of temporally different precipitation and potential evaporative effects on the
168 different reservoirs (e.g., Montanari et al., 2013). Teeth of large (>100 kg) obligate drinking
169 mammals record an average oxygen isotope composition of ingested waters ($\delta^{18}\text{O}_w$) from
170 different sources from a longer period. Thus the correlation between the average $\delta^{18}\text{O}$ values
171 of teeth enamel and the local precipitation is usually strong (Ayliffe et al., 1992; Bryant and

172 Froelich, 1995; Koch, 1998). However, there are exceptions for example glacial meltwaters,
173 rivers from mountainous area, or lakes with high evaporation in arid areas can have a
174 systematic $\delta^{18}\text{O}$ offset from the local precipitation. Migration of the animals can also
175 complicate the relationship. If animals migrated in order to escape harsh winters or to exploit
176 seasonally available resources, isotope composition of their enamel may not be representative
177 for the area where the fossils are found (Hoppe and Koch, 2007). The $\delta^{18}\text{O}$ values can also
178 offer information about the ecology of the different taxa if they lived under the same climatic
179 regime. Browsing taxa that ingest a higher proportion of ^{18}O -enriched water with their food
180 tend to have higher $\delta^{18}\text{O}$ values compared to sympatric grazing taxa (Kohn, 1996; Tütken et
181 al., 2013).

182 The oxygen isotope composition of local precipitation ($\delta^{18}\text{O}_{\text{ppt}}$) is controlled by several
183 factors. The mean annual temperature (MAT), the different moisture source, and air mass
184 trajectories, the latitude, altitude, continental and amount effects, all determine the isotopic
185 compositions of precipitation. The MAT generally has the greatest effect on the $\delta^{18}\text{O}$ values
186 of the precipitation ($\delta^{18}\text{O}_{\text{ppt}}$) at mid and high latitudes and in case of no extreme low or high
187 precipitation or humidity (Dansgaard, 1964; Rozanski et al., 1993).

188

189 *2.4. Pliocene-Pleistocene palaeoclimates and palaeoenvironments in Italy*

190

191 According to different proxies and models, the climate in the Early Pliocene was in general
192 warmer and wetter than today (2 – 3 °C higher global MAT with a decreased equator to pole
193 gradient) (Dowsett et al., 1996, 2013; Hill et al., 2011; Salzmann et al., 2011; Haywood et al.,
194 2013). In continental Europe thick forests were present with a temperate climate.
195 Palynological data suggest a relatively stable, warm-temperate climate in Northern Italy with
196 15 – 17 °C MAT and a MAP above 1000 mm (Bertini, 2001; 2010). Nevertheless, the slight

197 differences between mega-mesothermic elements and meso-microthermic ones suggest
198 modest fluctuations of temperature (Bertini, 2001). The Climatic Amplitude Method (CAM)
199 applied to other pollen records from Northern Italian sites gave MAT between 16 and 20 °C,
200 with the Most Likely Value (MLV) around 17 – 19 °C; and MAP between 1100 and 1500-
201 1600 mm, with the MLV around 1200 – 1300 mm (Fauquette et al., 1999, Fauquette and
202 Bertini, 2003, 2010). In Sicily the climate was warmer and drier (or with equal humidity) than
203 today (Fauquette et al., 1999, 2006; Combourieu-Nebout et al., 2015).

204 During the MN16a Neogene Mammalian biozone the climate in general became less stable
205 compared to the Early Pliocene (Hilgen et al., 2012). In SW Europe the modern
206 Mediterranean climatic regime was established and aridity was enhanced (Agustí et al., 2001;
207 Meyers and Hinnov, 2010; Rook and Martínez-Navarro, 2010; De Schepper et al., 2013,
208 2014; Woodard et al., 2014). The Villanyian/Villafranchian mammal turnover occurred at this
209 time in Europe and a renewal of archaic faunas to mammal assemblages with more modern
210 characteristics indicative to less humid environments under cooler climates documented also
211 in Italy (Pott, 1995; Bredenkamp et al., 2002; Petronio et al., 2011). From 3.3 to 3.0 Ma the
212 “Mid-Pliocene Warm Period” (MPWP) was characterised by 3 °C warmer global
213 temperatures, 10–40 m higher sea-level and less continental ice sheets compared to present
214 day, but even this stable, warm period was preceded by a short-lived, intense global glaciation
215 (3.305–3.285 Ma) (De Schepper et al., 2014). Around 3.3 Ma (MN16a, Triversa FU) in
216 Central Italy the faunas are characterized by the occurrence of new species and by the
217 diffusion of animals also adapted to open habitats. The palaeobotanical data indicates a
218 considerable homogeneity of the vegetation, at least in Northern Italy. Hence, besides the new
219 species, animals strictly relying on the forests still survived. For example *Anancus*
220 *arvernensis* as a forest living taxon survived from the Ruscinian.

221 At approximately 2.7 Ma the Northern Hemisphere Glaciation (NHG) occurred, followed by
222 glacial-interglacial cycles of moderate amplitude (orbital periodicity of 41 ka) (Dowsett et al.,
223 2013; Woodard et al., 2014; Salzmann et al., 2011, 2013; Haywood et al., 2013). The
224 resulting increase in aridity and more intense seasonality caused a replacement of forests by
225 tundra-like vegetation in Northern Europe (Pott, 1995; Bredenkamp et al., 2002) and a faunal
226 renewal in Italy, where several forest-dwelling taxa, especially small carnivores and arboreal-
227 scansorial taxa disappeared, whereas new large grazers, mixed feeders or even browsers
228 appeared. This renewal, called the “*Equus*-elephant event” can be regarded as a true turnover
229 phase (Palombo, 2007; Petronio et al., 2011). The irreversible transformation of the climate
230 regime determines rapid variations of the vegetation community, according to a repetitive
231 succession of vegetation types. This event also corresponds to a massive local disappearance
232 of thermophile and humidity-requiring woody plant taxa (Martinetto et al., 2015), even if a
233 few of them survived in Central Italy longer than in the rest of Europe (until the end of the
234 Gelasian, ca. 1.8 Ma), due to a combination of locally high precipitation and high
235 temperatures.

236 The entire interval between 2.5 and 1.0 Ma is characterized by relatively long interglacial
237 periods, with rather thick forest cover, and short glacial periods, with open vegetation in
238 Central and Southern Italy (Petronio et al., 2011 and references therein; Combourieu-Nebout
239 et al., 2015). In the Mediterranean area the typical glacial-interglacial cycles are characterized
240 by the succession of four main vegetation assemblages. Deciduous forest, subtropical/warm-
241 temperate forest, altitudinal conifer forest and open vegetation. This succession supports four
242 dominant climatic conditions: (1) a first increase of the temperature followed by (2) an
243 increase of the humidity, then (3) a decrease of temperature without variations of humidity
244 and (4) finally a strong decrease of the humidity, corresponding to a gradual transition from
245 warm and humid conditions during interglacials to cold and dry conditions during glacials

246 (Bertini, 2001, 2010). Pollen data indicate that the steppe-type of conditions, which are longer
247 lasting and more frequent in Southern Italy, developed only during some extreme glacial
248 peaks in Central Italy (Russo Ermolli et al., 2000; Pontini and Bertini, 2000; Petronio et al.,
249 2011). In North Italy the glacial periods led to a progressive expansion of a cooler forest-type
250 of vegetation cover (i.e., progressive increase of *Picea* and *Fagus*), but herbs including steppe
251 taxa remained a minor component (Bertini, 2001, 2010).

252 Despite the many variations it can be concluded that interglacial phases can be characterised
253 with high MAT and MAP, similar to that in the Zanclean, while during the glacial phases the
254 MAT and MAP were close to modern values. This cyclicity was controlled by the 41 ka
255 rhythm of the orbital periodicity continued in the entire period until 0.9 Ma (Bertini, 2000).

256 The Pliocene and Early Pleistocene sediments of Northern and Central Italy (often from the
257 same successions that yielded the studied fossil vertebrates) are rich in macrofossil plant
258 assemblages (Forno et al., 2015; Irace et al., 2015; Martinetto, 2015; Martinetto et al., 2015)
259 that have not yet been exploited for a thorough palaeoclimatic analysis, despite their
260 potentially very accurate indications (Teodoridis et al., 2015). The aims of this study are to
261 detect the temporal changes in the vegetation and in MAT and to compare the new isotope
262 results with the palaeobotanical proxies and palaeontological information. The comparisons
263 of the results obtained from the different approaches are summarized in Table 1.

264

265 **3. Materials and methods**

266

267 *3.1. Fossil materials*

268

269 Figure 1 and Table A1 give detailed information about the localities, their relative age
270 relationships and the types of investigated fossils. Altogether 51 fossils from 21 localities

271 were collected from the time period of about 5.2 to 1 Ma. For some localities only one sample
272 whereas for others up to 7 samples were collected. The fossils belong to four different
273 species, three of them are rhinocerotid: *Stephanorhinus etruscus* (n=21), "*Dihoplus*"
274 *megarhinus* (n=9), *Stephanorhinus jeanvireti* (n=6), and one proboscidean: *Anancus*
275 *arvernensis* (n=7) (Fig. 1, Table A1). These include rhinoceros samples that cannot be
276 determined at specific level (n=8). Wherever possible, teeth of adult individuals were
277 sampled. Each fossil probably represents a different individual. Samples were acquired from
278 the following institutions: DST, Department of Earth Science, Sapienza University of Roma
279 (Roma); MSNAF, Natural History Museum, Fisiocritici Academy, Siena (Siena); MGC,
280 Museum of Geology G. Capellini, (Bologna), MGPT, Museum of Geology and Paleontology,
281 University of Turin (Turin), MHMB, Natural History Museum Basel (Basel).

282 Many of the investigated sites and fossils are chronologically well calibrated using
283 magnetostratigraphy, cyclostratigraphy and biochronology. For the interpretation of the
284 results the samples were grouped in the Neogene Mammal biozones. The numbers of samples
285 from different time periods are different in Central and in North Italy. The oldest samples are
286 from MN14 in Central and from MN14-15 in North Italy. The precise stratigraphic and
287 geographic position of the "*Dihoplus*" *megarhinus* specimens from Dusino San Paolo is
288 uncertain; the MN14-15 interval is based on the well-known record of the taxa.

289 In Central Italy MNQ18, MNQ19 and MNQ19-20 biozones are treated separately, while in
290 the case of North Italy due to the fewer and less well-dated samples from these time periods,
291 the MN18-19-20 biozones are drawn together (n = 3). In North Italy the MN16 biozone can
292 be separated to MN16a (Triversa FU, 5 samples) and MNQ16b (Montopoli FU, 4 samples)
293 biozones. However recent analyses on plant macrofossils assemblages from the same area
294 where MNQ16b mammal assemblages have been reported, in NW Italy (Irace et al., 2015),
295 noted the absence of several thermophilous plants (HUTEA of Martinetto et al., 2015) already

296 within the latest Pliocene. This suggests a change of vegetation already in the late Pliocene,
297 and not only at the beginning of the Pleistocene. Since vegetation changes often coincide with
298 mammal turnover events, the actual assignment to the MN16a/MNQ16b mammal zones
299 should be further investigated. In fact the MNQ16b mammals are documented by 19th century
300 findings of uncertain stratigraphic position that could fall within the latest Pliocene as well as
301 within the earliest Pleistocene.

302

303 *3.2. Sampling*

304

305 After cleaning the surface mechanically, about 10 mg of bulk enamel was sampled from each
306 fossil using a Dremel diamond-studded drill. Where it was possible, enamel was sampled
307 along a vertical line over the whole enamel length from the crown to the root to get a
308 representative mean sample of the period of enamel formation. Due to sample limitations, in
309 some cases enamel from tooth fragments was collected. Because the complex process of
310 enamel formation and mineralization, which can be 2 – 3 years in the case of rhinos and
311 proboscideans, sampling enamel from a tooth fragment can still represent an average isotope
312 record of a longer period (Tafforeau et al., 2007; Metcalfe and Longstaffe, 2012). Where
313 possible, the teeth from adult individuals were sampled, because physiological effects such as
314 weaning/nursing can modify the $\delta^{13}\text{C}$ and $\delta^{18}\text{O}$ values of the bioapatite (Martin et al., 2008;
315 Metcalfe et al., 2010). Where possible, several samples were collected from each site to avoid
316 the effects of environmental factors and individual differences. According to Pryor et al.
317 (2014) typical uncertainty in temperature inferred from a single sample can be at least ± 4 °C,
318 while analyses of multiple samples can reduce the uncertainty to about 1 to 2 °C.

319

320 *3.3. Pre-treatment and measurements*

321

322 Sample powder was pre-cleaned according to the method given in Koch et al. (1997). NaOCl
323 was used to remove soluble organic material and acetic acid-Ca-acetate buffer to remove
324 exogenous carbonates (Koch et al., 1997; Kocsis, 2011). The pre-treatment methods have
325 been recently reviewed by Pellegrini and Snoeck (2016). The pre-treatment procedure
326 suggested is supported by the authors, but it is also clear that some unpredictable
327 contamination cannot be excluded. This may influence the finer crystalline material (e.g.,
328 bone, dentine) and could also be the cause for the slightly lower NBS-120c oxygen isotope
329 compositions measured parallel with the teeth.

330 After pre-cleaning, about 2 mg of sample was used for the carbonate isotopic measurements,
331 while for the $\delta^{18}\text{O}$ analyses, another 2 mg was dissolved and the phosphate ions were
332 precipitated as silver phosphate, according to methods adapted after Dettman et al. (2001) and
333 Kocsis (2011).

334 The carbon and oxygen isotopic compositions of structural carbonate were measured on a
335 Finnigan MAT Delta Plus XL mass spectrometer equipped with a GASBENCH-II preparation
336 unit. The samples were reacted with 99 % orthophosphoric acid and the produced CO_2 was
337 introduced to the mass spectrometer with He-carrier gas following procedures similar to those
338 described in Spötl and Vennemann (2003).

339 Carrara Marble in-house standards ($\delta^{18}\text{O} = -1.70$ ‰, VPDB; $\delta^{13}\text{C} = 2.05$ ‰, VPDB) were run
340 in the same sequence with the samples and used for correcting the data. The reproducibility of
341 the in-house standard is better than 0.1 ‰ (1σ) for both oxygen and carbon isotopic
342 compositions. NBS120c reference material (Florida phosphate rock) was treated and analysed
343 in parallel with the samples and gave values of $\delta^{13}\text{C}$ of -6.3 ± 0.1 ‰ (n=6) and $\delta^{18}\text{O}$ of $-2.3 \pm$
344 0.2 ‰ (n=6) on VPDB scale. These values are identical to those of the long-term average
345 values of NBS-120c in the laboratory.

346 For the phosphate $\delta^{18}\text{O}$ values the silver-phosphate was analysed via reduction with graphite
347 in a TC/EA (high-temperature conversion elemental analyser) coupled to a Finnigan MAT
348 Delta Plus XL mass spectrometer according to the values and method given in Vennemann et
349 al. (2002). The results were corrected to in-house Ag_3PO_4 phosphate standards (LK-2L: 12.1
350 ‰ and LK-3L: 17.9 ‰) that showed standard deviations (1σ) better than ± 0.3 ‰ during the
351 measurements. As internal standard the NBS-120c was prepared and run together with the
352 samples in order to test sample preparation. The analyses gave an average $\delta^{18}\text{O}$ value of 21.2
353 ± 0.3 ‰, (n=8), which is slightly lower than reported by others and also lower compared to the
354 NBS-120c that was measured for the calibration of TU-1 and TU-2 (21.7 ± 0.3 ‰, e.g.,
355 Vennemann et al., 2002; Halas et al., 2011). Because there is no internationally accepted $\delta^{18}\text{O}$
356 value for this material and as it is a sedimentary rock, the mammal teeth data were not
357 corrected further. The carbon isotope compositions are expressed relative to VPDB standard
358 (Vienna Pee Dee Belemnite), while the oxygen either to VPDB or VSMOW (Vienna Standard
359 Mean Ocean Water).

360

361 **4. Results**

362

363 The results of the carbon ($\delta^{13}\text{C}$) and oxygen ($\delta^{18}\text{O}_{\text{CO}_3}$ and $\delta^{18}\text{O}_{\text{PO}_4}$) isotope measurements
364 along with the calculated $\delta^{13}\text{C}$ values of vegetation, $\delta^{18}\text{O}$ values of environmental water
365 ($\delta^{18}\text{O}_w$) (see equations in Table 2) are presented in Table A1. The raw data, along with a step-
366 by-step set of calculations will allow a possible future verification and recalculation of the
367 results (recommendation of Skrzypek et al. 2016). Fig. 2 illustrates the $\delta^{13}\text{C}$ and $\delta^{18}\text{O}_{\text{PO}_4}$
368 values of the samples clustered in time bins with vegetation estimates and relative MAT
369 scales.

370 Most of the collected samples for this study have a $\delta^{18}\text{O}_{\text{CO}_3} - \delta^{18}\text{O}_{\text{PO}_4}$ offset between 7.2 ‰
371 and 10.6 ‰ (see in Table A1), which is typical for samples that have not been subjected to
372 diagenesis. Only two enamel samples have a lower carbonate-phosphate difference than 7.2
373 ‰, that is 6.8 and 6.9 ‰, which could indicate some degree of diagenetic alteration, but these
374 samples have similar phosphate $\delta^{18}\text{O}$ and carbonate $\delta^{13}\text{C}$ values as other samples from the
375 sites, so using these results does not change the site averages. It is possible that in these
376 samples the $\delta^{18}\text{O}_{\text{CO}_3}$ values were slightly affected by late diagenetic processes (e.g., exchange
377 with pore fluids).

378 To detect differences between species, MN biozones and areas, both parametric (F-tests for
379 variances and two-tailed homo- or heteroscedastic t-tests for central values) and non-
380 parametric (Levene tests for variances and two-tailed Mann-Whitney tests for central values)
381 statistical tests were made. One way ANOVA and non-parametric Kruskal-Wallis tests were
382 performed to compare variances of more than two groups. Statistical significance is based on
383 $p < 0.05$.

384

385 *4.1. Carbon isotope results*

386

387 The $\delta^{13}\text{C}$ values for the whole fauna range from -15.9 ‰ to -9.2 ‰ (VPDB). The range of
388 values is from -15.9 to -10.8 ‰ for Central Italy and from -15.1 to -9.2 ‰ for North Italy.
389 The three samples from South Italy from MNQ19 and MNQ20 vary between -12.1 and -11.5
390 ‰ (VPDB).

391 Two tailed homoscedastic t-test ($p = 0.92$) and Mann-Whitney test ($p = 0.75$) indicate that
392 there is no significant difference if all the values from Central and North Italy are compared.

393 The average values for the different time periods in Central and in North Italy are represented
394 in Fig. 2. There are significant differences between some time periods. In the case of Central

395 Italy t-tests indicate a change between MNQ18 and MNQ19 ($p = 0.044$) and between MNQ19
396 and MNQ19-20 ($p=0.014$). However, according to the Mann-Whitney test these differences
397 are not significant ($p = 0.125$ and $p = 0.092$). The average $\delta^{13}\text{C}$ values decrease by 1 ‰ from
398 MNQ18 to MNQ19 and increase by 2.3 ‰ from MNQ19 to MNQ19-20.

399 In the case of North Italy both t-test ($p=0.002$) and Mann-Whitney test ($p = 0.02$) support
400 changes between MN16a and MNQ16b. The change in average values is 2.1 ‰ in this
401 transition.

402 The four species have average $\delta^{13}\text{C}$ values between -14 ‰ and -13 ‰ with no difference
403 between them (ANOVA test, $p = 0.501$, Kruskal Wallis test, $p = 0.21$). The average values are
404 -13.0 ± 1.1 ‰ ($n = 21$) for *S. etruscus*; -13.9 ± 0.9 ‰ ($n = 9$) for "*D.*" *megarhinus*; -13.6 ± 1.3
405 ‰, ($n = 6$) for *S. jeanvireti*; and -13.9 ± 1.7 ‰ ($n=7$) for *A. arvernensis*.

406

407 4.2. $\delta^{18}\text{O}_{\text{PO}_4}$ value

408

409 The $\delta^{18}\text{O}_{\text{PO}_4}$ values for the whole fauna have a range from 12.0 to 18.7 ‰ (V-SMOW).
410 Regarding the regions, the values vary from 14.1 ‰ to 18.4 ‰ in Central Italy and from 12.0
411 ‰ to 15.7 ‰ in North Italy. The three samples from South Italy from MNQ19 and MNQ20
412 have values between 16.6 ‰ and 18.7 ‰. Comparing the average $\delta^{18}\text{O}_{\text{PO}_4}$ values from Central
413 and North Italy the difference is significant (t-test, $p=5.5 \times 10^{-6}$, Mann-Whitney test, $p =$
414 2.1×10^{-5}). In Central Italy the averages are higher than values of North Italy in all of the time
415 intervals. The differences are 1 – 3 ‰ with the highest difference in the MN14-15 biozone.
416 There are also differences in values between Central and South Italy in MNQ19-20. Samples
417 from South Italy have about 3 ‰ higher average $\delta^{18}\text{O}_{\text{PO}_4}$ values than samples from Central
418 Italy.

419 The average values for the different time periods in Central and in North Italy are represented
420 in Fig. 2. In Central Italy the average $\delta^{18}\text{O}_{\text{PO}_4}$ values decrease significantly from MN14 to
421 MN16 (t-test, $p = 0.004$, Mann-Whitney test, $p = 0.006$). In North Italy there are some
422 changes in the average values between the different biozones but these changes are not
423 significant.

424 The different species have the following average values: $15.5 \pm 1.5 \text{ ‰}$ ($n=21$) for *S. etruscus*;
425 $15.9 \pm 1.9 \text{ ‰}$ ($n=9$) for "*D.*" *megarhinus*; $15.7 \pm 0.7 \text{ ‰}$ ($n=7$) for *A. arvernensis* and 14.7 ± 0.9
426 ‰ ($n=6$) for *S. jeanvireti*. The three species have similar average values, while *S. jeanvireti*
427 has an average value about 1 ‰ lower. Differences among the species are not significant.

428

429 **5. Discussion**

430

431 *5.1 Palaeoenvironment, and diet of the taxa based on $\delta^{13}\text{C}$ values*

432

433 In this study all the $\delta^{13}\text{C}$ values indicate that these taxa were browsers or grazers in a pure C_3
434 ecosystem. It is compatible with earlier suggestions that C_4 grasses were absent in Europe
435 during the Pliocene to Late Pleistocene (Kürschner, 2010). Nonetheless, it must be mentioned
436 that Irace et al. (2015) reported the presence of C_4 sedges in NW Italy already in the latest
437 Pliocene. The ecology of the nearest living relatives (e.g. *Cyperus glomeratus*) suggests that
438 the distribution of these sedges was mainly limited to the disturbed environments along the
439 rivers, and there is no evidence permitting to reconstruct their frequency in the vegetation and
440 their possible importance as food for vertebrates (see Mishra et al., 2015).

441 Several calculations were made for the interpretation of the isotope results. The tested
442 equations are summarized in Table 2. From the $\delta^{13}\text{C}$ values the modern equivalent diet
443 composition are calculated and for this, the changes of the isotopic composition of

444 atmospheric CO₂ through time have to be taken into account. Based on isotopic data from
445 marine foraminifera, the reconstructed $\delta^{13}\text{C}$ value of the atmospheric CO₂ for the Pliocene is
446 about -6.3 ‰, ($\delta^{13}\text{C}_{\text{ancientatmCO}_2}$, Pliocene), for the Early Pleistocene it is about -6.5 ‰
447 ($\delta^{13}\text{C}_{\text{ancientatmCO}_2}$, Pleistocene), while the modern value was referenced to -8 ‰ ($\delta^{13}\text{C}_{\text{modernatm}}$,
448 year 2000, Kohn 2010), respectively (Tippie et al., 2010; Domingo et al., 2013). The modern
449 equivalent diet composition ($\delta^{13}\text{C}_{\text{diet,meq}}$) can be calculated with the equation of Domingo et al.
450 (2013) (Table 2.; Equation 1). Based on the expected $\delta^{13}\text{C}_{\text{diet, meq}}$ cut-off values for different
451 habitats by Domingo et al. (2013) our data indicate woodland to mesic C₃ grassland (-30 ‰
452 to -25 ‰) as a major flora type in Italy during the Pliocene. Some samples have lower values
453 suggesting the existence of closed-canopy forest but site averages are always higher than -30
454 ‰. There is only one sample that is slightly out of the above ranges (Lefte -23.7 ‰), where
455 probably local conditions were more enhanced. The value itself would fit the category of open
456 woodland-xeric C₃ grassland (-25 ‰ to -22 ‰) (Domingo et al., 2013).

457 The differences between $\delta^{13}\text{C}$ values could be the result of a complex combination of local
458 climatic control on the vegetation, habitat and dietary differences of the species. Measuring
459 samples from different taxa from the same location or the same species from different
460 locations would allow a better separation of these different controls. This separation is not
461 always possible due to sample limitations. For example, in this study all of the *S. jeanvireti*
462 samples are from the MN16 biozone and five of the six samples are from North Italy, so
463 different $\delta^{13}\text{C}$ values for this species could indicate dietary differences compared to the other
464 species and / or different climatic signal. Although the results must be interpreted with
465 caution, some implications of these differences can be considered.

466 Palaeontological observations of *A. arvernensis* suggest that it was a browser taxon that lived
467 in a forest or woodland (Kahlke et al., 2011; Rivals et al., 2015). Morphologically, the
468 bunodont molars generally imply a soft diet of leaves, fruits and twigs. Their feet were

469 adapted to walk on soft soil, also suggesting that it was an inhabitant of moist woodlands (Ji
470 et al., 2002; Rivals et al., 2015). The dentition changes in the fossil record imply a trend in its
471 diet from soft forest food towards the incorporation of grasses, requiring a grinding
472 component to mastication (Rivals et al., 2015). In agreement with the palaeontological
473 observations, the -13.9‰ average $\delta^{13}\text{C}$ values suggests that *A. arvernensis* lived in
474 woodlands. *S. jeanvireti* seems characteristic for a humid, forest-dominated environment with
475 relatively open areas where gramineous plants could be found (Guérin, 1972, 1980; Lacomat
476 and Mörs, 2008). *S. etruscus* has brachyodont dentition and slender, subcursorially structured
477 limbs (Guérin, 1980; Mazza, 1988) suggesting that this species probably inhabited
478 environments with variable forest cover similar to those in which black rhinos live today, i.e.
479 open scrub woodlands and the margins of small woods and feeding mainly on leaves, shrubs
480 and twigs (Guérin, 1980; Mazza, 1988; Fortelius et al., 1993). At Leffe, palynological and
481 faunal records of a lacustrine basin succession from approximately 1.8 to 1.1 Ma indicate
482 several environmental changes. The rhinoceros species (*S. etruscus* or *S. hundsheimiensis*)
483 lived in warm-temperate dense mixed or conifer forest, to open xerophytic communities and
484 steppe with tree birch and with sparse woodland patches (Ravazzi et al., 2009).

485 Overall, the palaeontological and environmental observations and the -13‰ to -13.9‰ $\delta^{13}\text{C}$
486 values are in agreement and suggest that all the investigated taxa could live in forested and
487 partly open environments and were browsers, feeding leaves, twigs shrubs and also grass if
488 these were present in the area. This could also imply that changes in measured $\delta^{13}\text{C}$ values
489 likely the effect of vegetation or climatic changes than change in food preference of the
490 animals.

491

492 *5.2. Environmental changes based on $\delta^{13}\text{C}$ data*

493

494 Variation in the measured $\delta^{13}\text{C}$ values in time and space depend on several factors, including
495 vegetation, precipitation and humidity and it is not always possible to separate these effects.
496 For example low $\delta^{13}\text{C}$ values could represent high precipitation and can indicate close canopy
497 forest, or both. However, temporal trends in $\delta^{13}\text{C}$ seem to reflect the environmental and
498 climatic changes in Italy from MN14 to MNQ20. A comparison of the $\delta^{13}\text{C}$ results and the
499 indications of palaeobotanical proxies can be seen in Table. 1.

500 The low $\delta^{13}\text{C}$ values in the Pliocene could represent high humidity, high precipitation values
501 and/or more closed woodlands in North and in Central Italy. The values remain the same in
502 Central Italy, where all the samples from MN16 biozone were averaged. In North Italy, where
503 the samples have a better age control, this biozone can be dissected; a sharp increase in $\delta^{13}\text{C}$
504 values between the late Pliocene and the early Pleistocene (MN16a – MN16b) is noted. The
505 1.9 ‰ increase in $\delta^{13}\text{C}$ values (Figure 2) could indicate vegetation changes from more closed
506 woodlands to more open areas and/or a large decrease in precipitation or in humidity. If only
507 the drop in MAP had an effect on the $\delta^{13}\text{C}$ values then this drop would be 1250 ± 630
508 mm/year according to the equation of Kohn (2010), (table 2., Equation 2., a latitude of 45°
509 and an altitude of 150m was substituted in the equation). The low $\delta^{13}\text{C}$ values in MN16a
510 probably reflect warm and humid climate of the “Mid-Pliocene Warm Period”, while the high
511 values in MNQ16b are most likely linked to the Northern Hemisphere Glaciation. This result
512 can confirm the considerable environmental changes also observed in palynological records
513 with an increase of a cooler type forest (*Picea* and *Fagus*) in North Italy (Stirone section) and
514 a vegetation opening in Central Italy around 2.6 Ma (Bertini, 2001, 2010).

515 Samples with younger ages are more common from the Central Italian area. Higher $\delta^{13}\text{C}$ for
516 the MNQ18 could indicate drier climate, less precipitation and / or more open vegetation
517 compared to previous biozones. This is in good agreement with pollen records, showing
518 decreased humidity at that time. After 2.6 Ma, the next indication of the vegetation change

519 may be noted for MNQ18 from 1.9 to 1.7 Ma in Central Italy (Bertini, 2001, 2010). During
520 MNQ19 (1.7 – 1.3 Ma) the $\delta^{13}\text{C}$ values decrease, which could represent wetter interglacial
521 periods and a more closed vegetation in the area. The youngest samples from MNQ19-20
522 (~1.2 Ma) from Madonna della Strada site show a more marked increase in $\delta^{13}\text{C}$ values.
523 Floral and faunal data suggest environments still characteristic of an interglacial between 1.3
524 and 1.1 Ma at this site (Magri et al., 2009). The recorded forest phase showed a clear
525 development, starting with an expansion of conifers, progressively replaced by a mixed oak
526 forest, and then showing an increase in Mediterranean vegetation. An appreciable diffusion of
527 open vegetation is also recorded, as indicated by pollen of grasses and other herbs. The finds
528 of *Mammuthus meridionalis* and “*Arvernoceros*” or *Eucladoceros giulii* also suggest the
529 presence of open environments. Overall the climate of the site could be similar to present day
530 climate, which is a semi-continental climate, with a transitional Mediterranean-temperate
531 character with about 700 mm precipitation (Magri et al., 2009).

532 From North Italy only three samples are presented from the younger biozones. These samples
533 from MNQ18-19-20 have higher average $\delta^{13}\text{C}$ values than samples from the Pliocene. The
534 sample from Leffe has the highest $\delta^{13}\text{C}$ value in the database (–9.2 ‰) indicating open
535 woodland-xeric grassland. As stated by Ravazzi et al. (2009), the observed variable forest
536 cover at the Leffe record documents the occurrence of the rhinoceros (*S. etruscus* or *S.*
537 *hundsheimiensis*) in cold-temperate, partially open environments, which is the coldest
538 extreme of Early Pleistocene climate cycles registered in the Biogenic Unit of the Leffe
539 Formation. According to this and the high $\delta^{13}\text{C}$ value, the sampled rhinoceros are presumably
540 from the younger part of the site and could live in a more open environment than the other
541 sampled taxa. However, as only one sample was analysed, the results are merely a suggestion
542 as seasonal effects can also be present and there could be individual differences between the
543 animals.

544 The average $\delta^{13}\text{C}$ values of the three samples from South Italy from MNQ19-20 (-13.8 ± 0.3
545 ‰) are similar to the values in Central and Northern Italy at that time and indicate partly open
546 vegetation.

547 Overall the temporal changes in $\delta^{13}\text{C}$ values in Italy are in good agreement with the pollen
548 data indicating that the changes in $\delta^{13}\text{C}$ reflect vegetation changes and / or changes in
549 precipitation or in humidity.

550

551 *5.3. Palaeotemperature changes derived from the $\delta^{18}\text{O}_{\text{PO}_4}$ data*

552

553 Estimating MAT from $\delta^{18}\text{O}_{\text{PO}_4}$ records require two data conversion steps that are based on
554 well-demonstrated correlations. The first is the correlation between the $\delta^{18}\text{O}_{\text{PO}_4}$ and the $\delta^{18}\text{O}$
555 values of consumed water (environmental water – $\delta^{18}\text{O}_w$), and the second is the correlation
556 between this $\delta^{18}\text{O}_w$ and the MAT of the site. Several uncertainties and assumptions are
557 inherent to both conversion steps. Different types of equations exist to calculate drinking
558 water of the animal from the $\delta^{18}\text{O}_{\text{PO}_4}$ data. General equations based on very large dataset often
559 show that the $\delta^{18}\text{O}_{\text{PO}_4}$ values of different species can have very similar offsets from the
560 drinking water. The species-specific equations, however, can be more reliable for the given
561 species with the given physiology.

562 There are more uncertainties in the second step regarding MAT. An assumption is needed for
563 the calculations, such that as the $\delta^{18}\text{O}$ of drinking water represents the $\delta^{18}\text{O}$ of the local mean
564 precipitation, which is not always the case (see effects of evaporation or meltwaters in
565 background section and below in the discussion) and that the estimate of past MAT can be
566 based on present day correlation between MAT and the isotope composition of precipitation.
567 There are local, regional and global equations for the datasets of one IAEA meteorological
568 station or for several stations worldwide. The advantage of using global equations is that they

569 represent an average mid-latitude climate regime and that they are not so sensitive to changes
570 in the local climates with time. Using site-specific precipitation-temperature relationships can,
571 however, give more precise estimates for a local area, notably if it is a mountainous area
572 where local climate variability may be important.

573 Amongst other influencing factors (different moisture source and air mass trajectories,
574 latitude, altitude, continental and amount effects) $\delta^{18}\text{O}$ of the local precipitation correlates
575 with the MAT. Due to this complex relationship, the correlation between the $\delta^{18}\text{O}$ and the
576 MAT is changing in time and space, and the correlation may be weak for non-continental or
577 monsoon-influenced stations. In these cases the type of the regression method and the type of
578 the dataset (monthly or annual average precipitation data) becomes an important factor and
579 could influence the palaeoclimatic interpretations (Pryor et al., 2014; Skrzypek et al., 2016).
580 There is currently a debate regarding the regression type to be used for palaeotemperature
581 reconstructions (see Pryor et al., 2014 vs. Skrzypek et al., 2016). Given the above
582 uncertainties, the relative changes in MAT were calculated in this study, instead of absolute
583 MAT values. Results of several equations were compared to observe the possible range of
584 MAT changes linked to the changes in $\delta^{18}\text{O}_{\text{PO}_4}$. The results were calculated using the
585 equations with the highest and the lowest slopes in both conversion steps. The equations used
586 are summarized in Table 2.

587 In the first step ($\delta^{18}\text{O}_{\text{PO}_4}$ to $\delta^{18}\text{O}_w$), different general equations (Kohn, 1996; Kohn and
588 Cerling 2002; Amiot et al., 2004) and one species-specific equation (Ayliffe, 1992; for
589 proboscidea) were used. In the second step ($\delta^{18}\text{O}_w$ to MAT) several regional and global
590 equations were compared: two equations for Europe (Pryor et al., 2014; Skrzypek et al.,
591 2016), and two global equations (Dansgaard, 1964; Amiot et al., 2004). Additionally a new
592 equation for Italy was produced based on the dataset of the Italian GNIP stations following
593 the work of Skrzypek et al. (2016). The R^2 of this regression is low, but the slope of the

594 equation is very similar to that of the regional and global equations. Equations with similar
595 slopes can be obtained for North and Central Italy as well.

596 The spatial distribution of the isotopic compositions of precipitation in present day Italy is
597 quite complex. Air masses from different origins have different $\delta^{18}\text{O}$ values and the
598 Apennines and the Alps also have an influence. Longinelli and Selmo (2002) found that the
599 relationship between the isotopic composition of precipitation and the mean monthly
600 temperature values are, on average, very poor. They found no latitudinal gradient along the
601 Tyrrhenian coast from Sicily to the Italian–French border, despite the considerable range of
602 latitude. However, there are 4–5 ‰ spatial differences in the isotopic composition of
603 precipitations and about 6–7 °C differences in MAT, as a result of the complex topography
604 and climate of Italy, there is not a simple south-north gradient.

605 The calculated MAT changes between MN14 and MNQ20 in Central Italy compared to other
606 proxies are shown in Table 1 and illustrated in Figure 2. The 1.4 ‰ decrease in $\delta^{18}\text{O}_{\text{PO}_4}$ values
607 from MN14 to MN16 can represent a 1.5 – 1.8 ‰ change in $\delta^{18}\text{O}_w$ and a 2 – 3.6 °C decrease
608 in MAT. The cooling trend from Early- to Late Pliocene –to Early Pleistocene is in good
609 agreement with indications of other proxies. Another decrease from MNQ18 to MNQ19-20 is
610 not significant, but with the average shift of –1.4 ‰ in $\delta^{18}\text{O}_{\text{PO}_4}$ could imply a similar 2 – 3.6
611 °C decrease in MAT. Because of the climate in MN19-20 (1.3 – 1.1 Ma) the Madonna della
612 Strada site was described as an interglacial with thermophilous taxa (Magri et al., 2009), it
613 can be assumed that during the glacial peaks in Early Pleistocene, temperature changes with
614 higher amplitude could have occurred.

615 In arid climates high evaporation of water reservoirs could raise the $\delta^{18}\text{O}$ values of the
616 animals' drinking water and thus the $\delta^{18}\text{O}_{\text{PO}_4}$ values. If the humidity changed with time,
617 calculations from the $\delta^{18}\text{O}_{\text{PO}_4}$ values would lead to over- or underestimation of MAT changes.

618 In this study for most of the time intervals the $\delta^{18}\text{O}_{\text{PO}_4}$ and $\delta^{13}\text{C}$ values appear to co-vary,

619 likely reflecting the warmer / wetter and cooler / more arid climates. However, some
620 exceptions, for example the MNQ19 zone in Central Italy, could be more humid and slightly
621 cooler than the previous mammal zone, which could imply that samples from that biozone are
622 from a different phase of a glacial-interglacial cycle. Low $\delta^{13}\text{C}$ values in most of the time
623 periods are in agreement with palaeobotanical proxies, indicating humid climates with dense
624 woodlands. In most of these conditions it is unlikely that strong evaporation could have led to
625 unusual ^{18}O enrichment in water and also phosphate. Some influence is only conceivable in
626 the case of the relatively cooler and more arid time periods such as MNQ18 in Central and
627 MNQ18-19-20 in North or in South Italy but in these cases the $\delta^{13}\text{C}$ values still indicate
628 woodlands so this effect should not be strong.

629 For Central Italy the decreasing temperatures from Early Pliocene to Late Pliocene – Early
630 Pleistocene followed by fluctuations but a long-term cooling trend towards the glacial-
631 interglacial cycles in Early Pleistocene are supported by the $\delta^{18}\text{O}_{\text{PO}_4}$ in the results and are in
632 agreement with other proxies.

633 In North Italy there are no large temporal changes in MAT. Whereas, the small increase in
634 $\delta^{18}\text{O}_{\text{PO}_4}$ values between MN14-MN15 and MN16a could be linked to the MPWP, while the
635 following decrease for the MNQ16b can refer to the NHG global cooling event. After this the
636 values stayed relatively constant for the younger time periods. The average $\delta^{18}\text{O}_{\text{PO}_4}$ values are
637 all lower than the values in Central Italy. The measured low $\delta^{18}\text{O}_{\text{PO}_4}$ values could suggest
638 colder MAT, especially during MN14-15, but would contradict other reported proxy data
639 (Fauquette et al., 1999, 2006, Bertini, 2001, 2010). In contrast, while samples from the end of
640 the Zanclean may well have lower $\delta^{18}\text{O}_{\text{PO}_4}$ compared to values from the warmest part of the
641 MPPW, the values being similar to MNQ18-19-20 are considered unlikely.

642 One explanation for the low $\delta^{18}\text{O}_{\text{PO}_4}$ values could be the influence of glacial meltwaters and
643 river waters draining from the Alps. This would have lower isotopic composition compared to

644 the local precipitation given an altitude effect on the catchment and/or a rain-shadow effect
645 with air mass transport dominated from the north. Therefore, drinking from water source
646 influenced by meltwater could have also lowered the $\delta^{18}\text{O}_{\text{PO}_4}$ values in the teeth. Isotope
647 measurements of waters from the upper part of the Po river support this assumption for a
648 present-day situation. The average composition of the river water is characterized by $\delta^{18}\text{O}$ of
649 -12.5‰ , while the $\delta^{18}\text{O}$ values of the precipitation are -7 to -9‰ in the same area (e. g.,
650 Marchina et al., 2014, Longinelli and Selmo, 2002). As in Central Italy trends in $\delta^{18}\text{O}_{\text{PO}_4}$
651 values are in agreement with other proxies, these local source-water effects, are considered
652 more likely compared to a regional-scale cooler climate. If it is the case, the $\delta^{18}\text{O}$ values in
653 North Italy could not be used for MAT calculations unless appropriate equations can be
654 deduced. Nonetheless, samples from more locations and broader time segments could
655 corroborate these hypotheses.

656 Palynological proxies indicate that the Zanclean MAT and precipitation were higher than the
657 Piacenzian, and the climate in North Italy was comparable to that of the other sites of the
658 north-western Mediterranean region (Table 1.). From the Piacenzian climatic and vegetation
659 characteristics of the middle European region have been suggested (Fauquette and Bertini,
660 2003). Mediterranean plants are poorly presented in the pollen records and totally lack in
661 plant macrofossil records (Martinetto, 2015 and unpublished data), while the persistence of
662 forests indicates constant humidity. Stable isotope measurements from the Carpathian Basin
663 also support similar results to those for North Italy in the given time period (e. g., Kovács et
664 al., 2015). For a present-day situation, an approximate 1 to 2 ‰ difference in $\delta^{18}\text{O}$ values in
665 precipitation and about 1 to 3 °C differences in MAT are given between areas near Torino and
666 Central Italy (e.g., Longinelli and Selmo, 2002, Combourieu-Nebout et al., 2015). It can be
667 concluded that about 1 to 2 ‰ lower $\delta^{18}\text{O}_{\text{ppt}}$ values in North Italy can be realistic compared to

668 Central Italy but larger differences may have an additional effect indicated, such as surface
669 waters from the Alpine catchments.

670 In South Italy the three samples from MNQ19-20 have higher $\delta^{18}\text{O}_{\text{PO}_4}$ values than samples
671 from Central Italy from this period. Two of the three samples are from the Pirro Nord site,
672 with very high values. This site is close to the Adriatic shore, closer than the other
673 investigated sites. Recent annual average $\delta^{18}\text{O}_{\text{ppt}}$ values in that area are about -5‰ , higher
674 than the -6 to -9‰ for other areas further from the sea, so the measured difference could be
675 the result of the shore-inland gradient in $\delta^{18}\text{O}_{\text{ppt}}$ values rather than a south-north temperature
676 gradient at that time (Longinelli and Selmo, 2003).

677

678 **6. Conclusions**

679

680 Stable isotope analyses of 51 enamel samples from fossil megaherbivores from North, Central
681 and South Italy (from 5.2 to about 1 Ma) provides information about the Pliocene and Early
682 Pleistocene climate in Italy. Most of the samples have a $\delta^{18}\text{O}_{\text{CO}_3} - \delta^{18}\text{O}_{\text{PO}_4}$ offsets between 7.2
683 to 10.6 ‰, which is compatible with a range typical for non-altered samples. All of the $\delta^{13}\text{C}$
684 values indicate that the investigated taxa lived in C_3 ecosystem. The $\delta^{13}\text{C}$ values support a
685 humid climate with woodlands during the Early Pliocene in North and in Central Italy. The
686 Northern Hemisphere Glaciation at 2.7 Ma is indicated as a sharp increase in $\delta^{13}\text{C}$ values
687 between MN16a and MNQ16b in North Italy. After MNQ16b the fluctuations probably
688 represent the moderate glacial-interglacial cycles with a long term increasing trend in $\delta^{13}\text{C}$
689 values. Higher values during MNQ18 and MNQ19-20 are in good agreement with pollen data
690 indicating more open vegetation. In Central Italy both stable isotope systems change in
691 tandem indicating warmer and more humid or cooler and more arid climates, respectively.
692 The $\delta^{18}\text{O}$ values support the warmest climate during the Early Pliocene followed by cooling

693 with fluctuations toward the end of the Early Pleistocene. In North Italy higher $\delta^{18}\text{O}_{\text{PO}_4}$ values
694 in MN16a are apparent – probably linked to the MPWP – but no other trends can be observed.
695 Attributing the low $\delta^{18}\text{O}_{\text{PO}_4}$ values in North Italy solely to MAT changes would result in low
696 MAT values during the Early Pliocene, in contrast to temperature changes inferred from other
697 proxies (Fauquette et al., 1999, 2006, Bertini, 2001, 2010). A possible explanation could be
698 that the drinking water was influenced by an Alpine catchment with typically lower mean
699 $\delta^{18}\text{O}$ values because of altitude and / or air mass origin differences for the northern parts of
700 Italy. With the exception of the low $\delta^{18}\text{O}$ values in North Italy, the Early Pliocene vegetation
701 and temperature changes fit well within the trends based on palynological records and
702 changes in mammal fossil assemblages.

703

704 **Acknowledgements**

705

706 The research has been generously funded by the Swiss SCIEX program Nr. 13.083. L.P.
707 thanks the European Commission's Research Infrastructure Action, EU-SYNTHESYS project
708 AT-TAF-2550, DE-TAF-3049, GB-TAF-2825, HU-TAF-3593, ES-TAF-2997; part of this
709 research received support from the SYNTHESYS Project <http://www.synthesys.info/> which is
710 financed by European Community Research Infrastructure Action under the FP7 "Capacities"
711 Program. The authors are grateful to Carlo Sarti (Museum of Geology G. Capellini, Bologna,
712 Italy), Daniele Ormezzano (Museum of Geology and Paleontology, University of Turin,
713 Turin, Italy), Ferruccio Farsi and Roberto Mazzei (Natural History Museum, Fisiocritici
714 Academy, Siena, Italy), Carmelo Petronio (Department of Earth Science, Sapienza,
715 University of Rome, Italy) and Loic Costeur (Natural History Museum Basel, Basel,
716 Switzerland) for supplying the fossil materials.

717

718 **References**

- 719 Agustí, J., Cabrera, L., Garcés, M., Krijgsman, W., Oms, O., Parés, J.M., 2001. A calibrated
720 mammal scale for the Neogene of Western Europe. State of the art. *Earth-Sci. Rev.* 52, 247-
721 260. [http://dx.doi.org/10.1016/S0012-8252\(00\)00025-8](http://dx.doi.org/10.1016/S0012-8252(00)00025-8)
- 722 Amiot, R., Lécuyer, C., Buffetaut, E., Fluteau, F., Legendre, S., Martineau, F., 2004.
723 Latitudinal temperature gradient during the Cretaceous Upper Campanian–Middle
724 Maastrichtian: $\delta^{18}\text{O}$ record of continental vertebrates. *Earth Planet. Sci. Lett.* 226, 255-272.
725 <http://dx.doi.org/10.1016/j.epsl.2004.07.015>
- 726 Arppe, L., Aaris-Sorensen, K., Daugnora, L., Lougas, L., Wojtal, P., Zupins, I., 2011. The
727 palaeoenvironmental delta C-13 record in European woolly mammoth tooth enamel. *Quat.*
728 *Int.* 245, 285-290. <http://dx.doi.org/10.1016/j.quaint.2010.10.018>
- 729 Arppe, L., Karhu, J.A., 2006. Implications for the Late Pleistocene climate in Finland and
730 adjacent areas from the isotopic composition of mammoth skeletal remains. *Palaeogeogr.*
731 *Palaeoclimatol. Palaeoecol.* 231, 322-330. <http://dx.doi.org/10.1016/j.palaeo.2005.08.007>
- 732 Arppe, L., Karhu, J.A., 2010. Oxygen isotope values of precipitation and the thermal climate
733 in Europe during the middle to late Weichselian ice age. *Quat. Sci. Rev.* 29, 1263-1275.
734 <http://dx.doi.org/10.1016/j.quascirev.2010.02.013>
- 735 Ayliffe, L.K., Chivas, A.R., Leakey, M.G., 1994. The retention of primary oxygen isotope
736 compositions of fossil elephant skeletal phosphate. *Geochim. Cosmochim. Acta* 58, 5291-
737 5298. [http://dx.doi.org/10.1016/0016-7037\(94\)90312-3](http://dx.doi.org/10.1016/0016-7037(94)90312-3)
- 738 Ayliffe, L.K., Lister, A.M., Chivas, A.R., 1992. The preservation of glacial-interglacial
739 climatic signatures in the oxygen isotopes of elephant skeletal phosphate. *Palaeogeogr.*
740 *Palaeoclimatol. Palaeoecol.* 99, 179-191. [http://dx.doi.org/10.1016/0031-0182\(92\)90014-v](http://dx.doi.org/10.1016/0031-0182(92)90014-v)
- 741 Balestrieri, M.L., Bernet, M., Brandon, M.T., Picotti, V., Reiners, P., Zattin, M., 2003.
742 Pliocene and Pleistocene exhumation and uplift of two key areas of the Northern Apennines.

743 Quat. Int. 101–102, 67-73. [http://dx.doi.org/10.1016/S1040-6182\(02\)00089-7](http://dx.doi.org/10.1016/S1040-6182(02)00089-7)

744 Bartolini, C., 2003. When did the Northern Apennine become a mountain chain? Quat. Int.
745 101–102, 75-80. [http://dx.doi.org/10.1016/S1040-6182\(02\)00090-3](http://dx.doi.org/10.1016/S1040-6182(02)00090-3)

746 Bertini, A., 2000. Pollen record from Colle Curti and Cesi: Early and Middle Pleistocene
747 mammal sites in the Umbro-Marchean Apennine Mountains (central Italy). J. Quat. Sci. 15,
748 825. [http://dx.doi.org/10.1002/1099-1417\(200012\)15:8<825::aid-jqs561>3.0.co;2-6](http://dx.doi.org/10.1002/1099-1417(200012)15:8<825::aid-jqs561>3.0.co;2-6)

749 Bertini, A., 2001. Pliocene climatic cycles and altitudinal forest development from 2.7 Ma in
750 the Northern Apennines (Italy): Evidence from the pollen record of the Stirone section (~ 5.1
751 to ~ 2.2 Ma). Geobios 34, 253-265. [http://dx.doi.org/10.1016/S0016-6995\(01\)80074-7](http://dx.doi.org/10.1016/S0016-6995(01)80074-7)

752 Bertini, A., 2010. Pliocene to Pleistocene palynoflora and vegetation in Italy: State of the art.
753 Quat. Int. 225, 5-24. <http://dx.doi.org/10.1016/j.quaint.2010.04.025>

754 Bianucci, G., Mazza, P., Merla, D., Sarti, G. & Cascella, A., 2001. The early Pliocene
755 mammal assemblage of Val di Pugna (Tuscany, Italy) in the light of calcareous plankton
756 biostratigraphical data and paleoecological observations. Riv. Ital. Paleontol. S., 107, 425-438.

757 Blake, R.E., Oneil, J.R., Garcia, G.A., 1997. Oxygen isotope systematics of biologically
758 mediated reactions of phosphate .1. Microbial degradation of organophosphorus compounds.
759 Geochim. Cosmochim. Acta 61, 4411-4422. [http://dx.doi.org/10.1016/s0016-7037\(97\)00272-](http://dx.doi.org/10.1016/s0016-7037(97)00272-)
760 x

761 Bocherens, H., Pacaud, G., Lazarev, P.A., Mariotti, A., 1996. Stable isotope abundances (C-
762 13, N-15) in collagen and soft tissues from Pleistocene mammals from Yakutia: Implications
763 for the palaeobiology of the Mammoth Steppe. Palaeogeogr. Palaeoclimatol. Palaeoecol. 126,
764 31-44. [http://dx.doi.org/10.1016/s0031-0182\(96\)00068-5](http://dx.doi.org/10.1016/s0031-0182(96)00068-5)

765 Bredenkamp, G.J., Spada, F., Kazmierczak, E., 2002. On the origin of northern and southern
766 hemisphere grasslands. Plant Ecol. 163, 209-229. <http://dx.doi.org/10.1023/a:1020957807971>

767 Bruhl, J.J., Wilson, K.L., 2007. Towards a Comprehensive Survey of C3 and C4

768 Photosynthetic Pathways in Cyperaceae. *Aliso* 23, 99–148.
769 <http://scholarship.claremont.edu/aliso/vol23/iss1/11>

770 Bryant, J.D., Froelich, P.N., 1995. A model of oxygen isotope fractionation in body water of
771 large mammals. *Geochim. Cosmochim. Acta* 59, 4523-4537. [http://dx.doi.org/10.1016/0016-](http://dx.doi.org/10.1016/0016-7037(95)00250-4)
772 [7037\(95\)00250-4](http://dx.doi.org/10.1016/0016-7037(95)00250-4)

773 Bryant, J.D., Koch, P.L., Froelich, P.N., Showers, W.J., Genna, B.J., 1996. Oxygen isotope
774 partitioning between phosphate and carbonate in mammalian apatite. *Geochim. Cosmochim.*
775 *Acta* 60, 5145-5148. [http://dx.doi.org/10.1016/S0016-7037\(96\)00308-0](http://dx.doi.org/10.1016/S0016-7037(96)00308-0)

776 Cerling, T.E., Harris, J.M., 1999. Carbon isotope fractionation between diet and bioapatite in
777 ungulate mammals and implications for ecological and paleoecological studies. *Oecologia*
778 120, 347-363. <http://dx.doi.org/10.1007/s004420050868>

779 Clauss, M., Polster, C., Kienzle, E., Wiesner, H., Baumgartner, K., von Houwald, F., Streich,
780 W.J., Dierenfeld, E., 2005. Energy and mineral nutrition and water intake in the captive
781 Indian rhinoceros (*Rhinoceros unicornis*). *Zoo Biol.* 24, 1-14.
782 <http://dx.doi.org/10.1002/zoo.20032>

783 Clementz, M.T., 2012. New insight from old bones: stable isotope analysis of fossil
784 mammals. *J. Mammal.* 93, 368-380. <http://dx.doi.org/10.1644/11-mamm-s-179.1>

785 Coltorti, M., Pieruccinia, P., Rustioni, M., 2008. The Barga Basin (Tuscany): A record of
786 Plio-Pleistocene mountain building of the Northern Apennines, Italy. *Quat. Int.*, 189, 56–70.

787 Combourieu-Nebout, N., Bertini, A., Russo-Ermolli, E., Peyron, O., Klotz, S., Montade, V.,
788 Fauquette, S., Allen, J., Fusco, F., Goring, S., Huntley, B., Joannin, S., Lebreton, V., Magri,
789 D., Martinetto, E., Orain, R., Sadori, L., 2015. Climate changes in the central Mediterranean
790 and Italian vegetation dynamics since the Pliocene. *Rev. Paleobot. Palyno.* 218, 127-147.
791 <http://dx.doi.org/10.1016/j.revpalbo.2015.03.001>

792 Crowley, B.E., Wheatley, P.V., 2014. To bleach or not to bleach? Comparing treatment

793 methods for isolating biogenic carbonate. *Chem. Geol.* 381, 234-242.
794 <http://dx.doi.org/10.1016/j.chemgeo.2014.05.006>

795 Dansgaard, W., 1964. Stable isotopes in precipitation. *Tellus* 16, 436-468. [http://dx.doi.org/](http://dx.doi.org/10.1111/j.2153-3490.1964.tb00181.x)
796 [10.1111/j.2153-3490.1964.tb00181.x](http://dx.doi.org/10.1111/j.2153-3490.1964.tb00181.x)

797 De Schepper, S., Gibbard, P.L., Salzmann, U., Ehlers, J., 2014. A global synthesis of the
798 marine and terrestrial evidence for glaciation during the Pliocene Epoch. *Earth-Sci. Rev.* 135,
799 83-102. <http://dx.doi.org/10.1016/j.earscirev.2014.04.003>

800 De Schepper, S., Groeneveld, J., Naafs, B.D.A., Van Renterghem, C., Hennissen, J., Head,
801 M.J., Louwe S, Fabian K. 2013. Northern Hemisphere Glaciation during the Globally Warm
802 Early Late Pliocene. *Plos One* 8. (12): e81508,
803 <http://dx.doi.org/10.1371/journal.pone.0081508>

804 Dettman, D.L., Kohn, M.J., Quade, J., Ryerson, F.J., Ojha, T.P., Hamidullah, S., 2001.
805 Seasonal stable isotope evidence for a strong Asian monsoon throughout the past 10.7 m.y.
806 *Geology* 29, 31-34. [http://dx.doi.org/10.1130/0091-7613\(2001\)029<0031:ssiefa>2.0.co;2](http://dx.doi.org/10.1130/0091-7613(2001)029<0031:ssiefa>2.0.co;2)

807 Domingo, L., Koch, P.L., Hernandez Fernandez, M., Fox, D.L., Domingo, M.S., Teresa
808 Alberdi, M., 2013. Late Neogene and Early Quaternary Paleoenvironmental and Paleoclimatic
809 Conditions in Southwestern Europe: Isotopic Analyses on Mammalian Taxa. *Plos One* 8,
810 e63739, <http://dx.doi.org/10.1371/journal.pone.0063739>

811 Dowsett, H., Barron, J., Poore, R., 1996. Middle Pliocene sea surface temperatures: a global
812 reconstruction. *Mar. Micropaleontol.* 27, 13-25. [http://dx.doi.org/10.1016/0377-](http://dx.doi.org/10.1016/0377-8398(95)00050-X)
813 [8398\(95\)00050-X](http://dx.doi.org/10.1016/0377-8398(95)00050-X)

814 Dowsett, H.J., Foley, K.M., Stoll, D.K., Chandler, M.A., Sohl, L.E., Bentsen, M., Otto-
815 Bliesner, B.L., Bragg, F.J., Chan, W.L., Contoux, C., Dolan, A.M., Haywood, A.M., Jonas,
816 J.A., Jost, A., Kamae, Y., Lohmann, G., Lunt, D.J., Nisancioglu, K.H., Abe-Ouchi, A.,
817 Ramstein, G., Riesselman, C.R., Robinson, M.M., Rosenbloom, N.A., Salzmann, U.,

818 Stepanek, C., Strother, S.L., Ueda, H., Yan, Q., Zhang, Z.S., 2013. Sea Surface Temperature
819 of the mid-Piacenzian Ocean: A Data-Model Comparison. *Scientific Reports* 3, article
820 number 2013. <http://dx.doi.org/10.1038/srep02013>

821 Drucker, D.G., Bridault, A., Hobson, K.A., Szuma, E., Bocherens, H., 2008. Can carbon-13 in
822 large herbivores reflect the canopy effect in temperate and boreal ecosystems? Evidence from
823 modern and ancient ungulates. *Palaeogeogr. Palaeoclimatol. Palaeoecol. Palaeogeogr.*
824 *Palaeoclimatol. Palaeoecol.* 266, 69-82. <http://dx.doi.org/10.1016/j.palaeo.2008.03.020>

825 Farquhar, G.D., Ehleringer, J.R., Hubick, K.T., 1989. Carbon Isotope Discrimination and
826 Photosynthesis. *Annu. Rev. Plant. Phys.* 40, 503-537. [http://dx.doi.org/](http://dx.doi.org/10.1146/annurev.pp.40.060189.002443)
827 [10.1146/annurev.pp.40.060189.002443](http://dx.doi.org/10.1146/annurev.pp.40.060189.002443)

828 Fauquette, S., Bertini, A., 2003. Quantification of the northern Italy Pliocene climate from
829 pollen data: evidence for a very peculiar climate pattern. *Boreas* 32, 361-369.
830 [http://dx.doi.org/ 10.1080/03009480310002235](http://dx.doi.org/10.1080/03009480310002235)

831 Fauquette, S., Suc, J.P., Bertini, A., Popescu, S.M., Warny, S., Taoufiq, N.B., Villa, M.J.P.,
832 Chikhi, H., Feddi, N., Subally, D., Clauzon, G., Ferrier, J., 2006. How much did climate force
833 the Messinian salinity crisis? Quantified climatic conditions from pollen records in the
834 Mediterranean region. *Palaeogeogr. Palaeoclimatol. Palaeoecol.* 238, 281-301.
835 [http://dx.doi.org/ 10.1016/j.palaeo.2006.03.029](http://dx.doi.org/10.1016/j.palaeo.2006.03.029)

836 Fauquette, S., Suc, J.P., Guiot, J., Diniz, F., Feddi, N., Zheng, Z., Bessais, E., Drivaliari, A.,
837 1999. Climate and biomes in the West Mediterranean area during the Pliocene. *Palaeogeogr.*
838 *Palaeoclimatol. Palaeoecol.* 152, 15-36. [http://dx.doi.org/ 10.1016/s0031-0182\(99\)00031-0](http://dx.doi.org/10.1016/s0031-0182(99)00031-0)

839 Feranec, R.S., 2004. Geographic variation in the diet of hypsodont herbivores from the
840 Rancholabrean of Florida. *Palaeogeogr. Palaeoclimatol. Palaeoecol.* 207, 359-369.
841 [http://dx.doi.org/ 10.1016/j.palaeo.2003.09.031](http://dx.doi.org/10.1016/j.palaeo.2003.09.031)

842 Feranec, R.S., MacFadden, B.J., 2006. Isotopic discrimination of resource partitioning among

843 ungulates in C-3-dominated communities from the Miocene of Florida and California.
844 *Paleobiology* 32, 191-205. <http://dx.doi.org/10.1666/05006.1>

845 Fondi, R., 2007. Introduzione alla conoscenza dei mammiferi del Plio-Pleistocene italiano. II:
846 Proboscidi. *Etrurianatura* 2, 40-50.

847 Forno, M.G., Gattiglio, M., Comina, C., Barbero, D., Bertini, A., Doglione, A., Gianotti, F.,
848 Irace, A., Martinetto, M., Mottura, A., Sala, B., 2015. Stratigraphic and tectonic notes on the
849 Villafranca d'Asti succession in the type-area and Castelnuovo Don Bosco sector (Asti reliefs,
850 Piedmont). *A.M.Q.* 28, 5-27.

851 Fortelius, M., Eronen, J., Liu, L.P., Pushkina, D., Tesakov, A., Vislobokova, I., Zhang, Z.Q.,
852 2006. Late Miocene and Pliocene large land mammals and climatic changes in Eurasia.
853 *Palaeogeogr. Palaeoclimatol. Palaeoecol.* 238, 219-227.
854 <http://dx.doi.org/10.1016/j.palaeo.2006.03.042>

855 Fricke, H.C., Clyde, W.C., O'Neil, J.R., 1998. Intra-tooth variations in delta O-18 (PO4) of
856 mammalian tooth enamel as a record of seasonal variations in continental climate variables.
857 *Geochim. Cosmochim. Acta* 62, 1839-1850. [http://dx.doi.org/10.1016/s0016-7037\(98\)00114-](http://dx.doi.org/10.1016/s0016-7037(98)00114-8)
858 8.

859 García-Alix, A., 2015. A multiproxy approach for the reconstruction of ancient continental
860 environments. The case of the Mio–Pliocene deposits of the Granada Basin (southern Iberian
861 Peninsula). *Glob. Planet. Change* 131, 1-10.
862 <http://dx.doi.org/10.1016/j.gloplacha.2015.04.005>

863 Guérin, C., 1972. Une nouvelle espèce de Rhinocéros (Mammalia, Perissodactyla) à Vialette
864 (Haute-Loire, France) et dans d'autres gisements du Villafranchien Inférieur Européen:
865 *Dicerorhinus jeanvireti* n. sp.. Documents des Laboratoires de Géologie de la Faculté des
866 Sciences de Lyon 49, 53-161.

867 Guérin, C., 1980. Les rhinocéros (Mammalia, Perissodactyla) du Miocène terminal au

868 Pléistocène supérieur en Europe occidentale. Comparaison avec les espèces actuelles.
869 Documents du Laboratoire de Géologie de la Faculté des Sciences de Lyon 79, 1-1183.
870 Halas, S., Skrzypek, G., Meier-Augenstein, W., Pelc, A., Kemp, H.F., 2011. Inter-laboratory
871 calibration of new silver orthophosphate comparison materials for the stable oxygen isotope
872 analysis of phosphates. *Rapid Commun. Mass Spectrom.* 25, 579-84.
873 <http://dx.doi.org/10.1002/rcm.4892>
874 Hartman, G., Bar-Yosef, O., Brittingham, A., Grosman, L., Munro, N.D., 2016. Hunted
875 gazelles evidence cooling, but not drying, during the Younger Dryas in the southern Levant.
876 *Proc. Natl. Acad. Sci.* 113, 3997-4002. <http://dx.doi.org/10.1073/pnas.1519862113>
877 Haywood, A.M., Hill, D.J., Dolan, A.M., Otto-Bliesner, B.L., Bragg, F., Chan, W.L.,
878 Chandler, M.A., Contoux, C., Dowsett, H.J., Jost, A., Kamae, Y., Lohmann, G., Lunt, D.J.,
879 Abe-Ouchi, A., Pickering, S.J., Ramstein, G., Rosenbloom, N.A., Salzmann, U., Sohl, L.,
880 Stepanek, C., Ueda, H., Yan, Q., Zhang, Z., 2013. Large-scale features of Pliocene climate:
881 results from the Pliocene Model Intercomparison Project. *Clim. Past* 9, 191-209.
882 <http://dx.doi.org/10.5194/cp-9-191-2013>
883 Hilgen, F.J., Lourens, L.J., Van Dam, J.A., Beu, A.G., Boyes, A.F., Cooper, R.A., Krijgsman,
884 W., Ogg, J.G., Piller, W.E., Wilson, D.S., 2012. The Neogene Period, in: Gradstein, F.M.,
885 Schmitz, J.G.O.D., Ogg, G.M. (Eds.), *The Geologic Time Scale*. Elsevier, Boston, pp. 923–
886 978.
887 Hill, D.J., Csank, A.Z., Dolan, A.M., Lunt, D.J., 2011. Pliocene climate variability: Northern
888 Annular Mode in models and tree-ring data. *Palaeogeogr. Palaeoclimatol. Palaeoecol.* 309,
889 118-127. <http://dx.doi.org/10.1016/j.palaeo.2011.04.003>
890 Iacumin, P., Bocherens, H., Mariotti, A., Longinelli, A., 1996. Oxygen isotope analyses of co-
891 existing carbonate and phosphate in biogenic apatite: A way to monitor diagenetic alteration
892 of bone phosphate? *Earth Planet. Sci. Lett.* 142, 1-6. <http://dx.doi.org/10.1016/0012->

893 821x(96)00093-3

894 Hoppe, K.A., Koch, P.L., 2007. Reconstructing the migration patterns of late Pleistocene
895 mammals from northern Florida, USA. *Quat. Res.* 68, 347-352.
896 <http://dx.doi.org/10.1016/j.yqres.2007.08.001>

897 Iacumin, P., Nikolaev, V., Ramigni, M., 2000. C and N stable isotope measurements on
898 Eurasian fossil mammals, 40 000 to 10 000 years BP: Herbivore physiologies and
899 palaeoenvironmental reconstruction. *Palaeogeogr. Palaeoclimatol. Palaeoecol.* 163, 33-47.
900 [http://dx.doi.org/10.1016/s0031-0182\(00\)00141-3](http://dx.doi.org/10.1016/s0031-0182(00)00141-3)

901 Irace, A., Monegato, G., Tema, E., Martinetto, E., Gianolla, D., Vassio, E., Bellino, L.,
902 Violanti, D., 2015. Unconformity-bounded stratigraphy in the Plio-Pleistocene continental
903 record: new insights from the Alessandria Basin (NW Italy). *Geol. J.* 2015[Published online].
904 <http://dx.doi.org/10.1002/gj.2744>

905 Ji, Q., Luo, Z-X., Yuan, C-X., Wible, J.R., Zhang, J-P., Georgi, J.A., 2002. The earliest
906 known eutherian mammal. *Nature* 416, 816-822. <http://dx.doi.org/10.1038/416816a>

907 Kahlke, R-D., García, N., Kostopoulos, D.S., Lacombat, F., Lister, A.M., Mazza, P.P.A.,
908 Spassov, N., Titov, V.V., 2011. Western Palaeartic palaeoenvironmental conditions during
909 the Early and early Middle Pleistocene inferred from large mammal communities, and
910 implications for hominin dispersal in Europe. *Quat, Sci. Rev.* 30, 1368-1395.
911 <http://dx.doi.org/10.1016/j.quascirev.2010.07.020>

912 Klotz, S., Fauquette, S., Combourieu-Nebout, N., Uhl, D., Suc, J-P., Mosbrugger, V., 2006.
913 Seasonality intensification and long-term winter cooling as a part of the Late Pliocene climate
914 development. *Earth Planet. Sci. Lett.* 241, 174-187. DOI:
915 <http://dx.doi.org/10.1016/j.epsl.2005.10.005>

916 Koch, P.L., 1998. Isotopic reconstruction of past continental environments. *Annu. Rev. Earth*
917 *Planet. Sci.* 26, 573-613. <http://dx.doi.org/10.1146/annurev.earth.26.1.573>

918 Koch, P.L., Tuross, N., Fogel, M.L., 1997. The effects of sample treatment and diagenesis on
919 the isotopic integrity of carbonate in biogenic hydroxylapatite. *J. Archaeol. Sci.* 24, 417-429.
920 <http://dx.doi.org/10.1006/jasc.1996.0126>

921 Kocsis, L., 2011. Geochemical Compositions of Marine Fossils as Proxies for Reconstructing
922 Ancient Environmental Conditions. *Chimia* 65, 787-791.
923 <http://dx.doi.org/10.2533/chimia.2011.787>

924 Kocsis, L., Ozsvart, P., Becker, D., Ziegler, R., Scherler, L., Codrea, V., 2014. Orogeny
925 forced terrestrial climate variation during the late Eocene-early Oligocene in Europe. *Geology*
926 42, 727-730. <http://dx.doi.org/10.1130/g35673.1>

927 Kohn, M.J., 1996. Predicting animal delta O-18: Accounting for diet and physiological
928 adaptation. *Geochim. Cosmochim. Acta* 60, 4811-4829. [http://dx.doi.org/10.1016/s0016-](http://dx.doi.org/10.1016/s0016-7037(96)00240-2)
929 [7037\(96\)00240-2](http://dx.doi.org/10.1016/s0016-7037(96)00240-2)

930 Kohn MJ. 2010. Carbon isotope compositions of terrestrial C3 plants as indicators of
931 (paleo)ecology and (paleo)climate. *Proc. Natl. Acad. Sci.* 107, 19691-19695. DOI:
932 [10.1073/pnas.1004933107](https://doi.org/10.1073/pnas.1004933107)

933 Kohn, M.J., Cerling, T.E., 2002. Stable isotope compositions of biological apatite. *Rev.*
934 *Mineral. Geochem.* 48, 455–488. <http://dx.doi.org/10.2138/rmg.2002.48.12>

935 Kohn, M.J., Schoeninger, M.J., Barker, W.W., 1999. Altered states: Effects of diagenesis on
936 fossil tooth chemistry. *Geochim. Cosmochim. Acta* 63, 2737-2747.
937 [http://dx.doi.org/10.1016/s0016-7037\(99\)00208-2](http://dx.doi.org/10.1016/s0016-7037(99)00208-2).

938 Kotsakis, T., 1986. Elementi di paleobiogeografia dei mammiferi terziari dell'Italia. *Hystrix*,
939 1, 25-68.

940 Kotsakis, T., Barisone, G., 2008. I vertebrati fossili continentali del Plio-Pleistocene dell'area
941 Romana, in: Funiciello, R., Praturlon, A., Giordano, G. (Eds.), *La Geologia Di Roma*,
942 *Memorie Descrittive della Carta Geologica d'Italia* 80, 115–143.

943 Kotsakis, T., Pandolfi, L., 2012. The Plio-Pleistocene Mammal Assemblages from the Intra-
944 Apennine Basins. *Rendiconti Online della Società Geologica Italiana* 23, 69-76.

945 Kovács, J., Szabó, P., Kocsis, L., Vennemann, T., Sabol, M., Gasparik, M., Virág, A., 2015.
946 Pliocene and Early Pleistocene paleoenvironmental conditions in the Pannonian Basin
947 (Hungary, Slovakia): Stable isotope analyses of fossil proboscidean and perissodactyl teeth.
948 *Palaeogeogr. Palaeoclimatol. Palaeoecol.* 440, 455-
949 466. <http://dx.doi.org/10.1016/j.palaeo.2015.09.019>

950 Kürschner, W.M., 2010. C-isotope composition of fossil sedges and grasses. *Geophys. Res.*
951 *Abstr.* 12, EGU2010-8012-1.

952 Lacombat, F., Mors, T., 2008. The northernmost occurrence of the rare Late Pliocene
953 rhinoceros *Stephanorhinus jeanvireti* (Mammalia, Perissodactyla). *Neues Jahrb. Geol. P-A.*
954 249, 157-165. <http://dx.doi.org/10.1127/0077-7749/2008/0249-0157>

955 Leethorp, J.A., Sealy, J.C., Vandermerwe, N.J., 1989. Stable carbon isotope ratio differences
956 between bone collagen and bone apatite, and their relationship to diet. *J. Archaeol. Sci.* 16,
957 585-599. [http://dx.doi.org/10.1016/0305-4403\(89\)90024-1](http://dx.doi.org/10.1016/0305-4403(89)90024-1)

958 Levin, N.E., Cerling, T.E., Passey, B.H., Harris, J.M., Ehleringer, J.R., 2006. A stable isotope
959 aridity index for terrestrial environments. *Proc. Natl. Acad. Sci.* 103, 11201-11205.
960 <http://dx.doi.org/10.1073/pnas.0604719103>

961 Liang, Y., Blake, R.E., 2007. Oxygen isotope fractionation between apatite and aqueous-
962 phase phosphate: 20-45 degrees C. *Chem. Geol.* 238, 121-133.
963 <http://dx.doi.org/10.1016/j.chemgeo.2006.11.004>

964 Loftus, E., Stewart, B.A., Dewar, G., Lee-Thorp, J., 2015. Stable isotope evidence of late MIS
965 3 to middle Holocene palaeoenvironments from Sehonghong Rockshelter, eastern Lesotho. *J.*
966 *Quat. Sci.* 30, 805-816. <http://dx.doi.org/10.1002/jqs.2817>

967 Longinelli, A., 1984. Oxygen isotopes in mammal bone phosphate: A new tool for

968 paleohydrological and paleoclimatological research? *Geochim. Cosmochim. Acta* 48, 385-
969 390. [http://dx.doi.org/10.1016/0016-7037\(84\)90259-x](http://dx.doi.org/10.1016/0016-7037(84)90259-x)

970 Loss, R., 1945. Resti di *Rhinoceros* dalla località Becchi di Castelnuovo San Bosco (Colle
971 San Bosco, Torino). *Natura* 36, 63-70.

972 Luz, B., Cormie, A.B., Schwarcz, H.P., 1990. Oxygen isotope variations in phosphate of deer
973 bones. *Geochim. Cosmochim. Acta* 54, 1723-1728. [http://dx.doi.org/10.1016-](http://dx.doi.org/10.1016/0016-7037(90)90403-8)
974 [7037\(90\)90403-8](http://dx.doi.org/10.1016/0016-7037(90)90403-8)

975 Luz, B., Kolodny, Y., 1985. Oxygen isotope variations in phosphate of biogenic apatites. 4.
976 Mammal teeth and bones. *Earth Planet. Sci. Lett.* 75, 29-36. [http://dx.doi.org/10.1016/0012-](http://dx.doi.org/10.1016/0012-821x(85)90047-0)
977 [821x\(85\)90047-0](http://dx.doi.org/10.1016/0012-821x(85)90047-0)

978 Luz, B., Kolodny, Y., Horowitz, M., 1984. Fractionation of oxygen isotopes between
979 mammalian bone-phosphate and environmental drinking water. *Geochim. Cosmochim. Acta*
980 48, 1689-1693. [http://dx.doi.org/10.1016/0016-7037\(84\)90338-7](http://dx.doi.org/10.1016/0016-7037(84)90338-7)

981 Magri, D., Di Rita, F., Palombo, M.R., 2010. An Early Pleistocene interglacial record from an
982 intermontane basin of central Italy (Scoppito, L'Aquila). *Quat. Int.* 225, 106-113.
983 <http://dx.doi.org/10.1016/j.quaint.2009.04.005>

984 Mancini, M., Cavuoto, G., Pandolfi, L., Petronio, C., Salari, L., Sardella, R., 2012. Coupling
985 basin infill history and mammal biochronology in a Pleistocene intramontane basin: The case
986 of western L'Aquila Basin (central Apennines, Italy). *Quat. Int.* 267, 62-77.
987 <http://dx.doi.org/10.1016/j.quaint.2011.03.020>

988 Marchina, C., Bianchini, G., Natali, C., Pennisi, M., Colombani, N., Tassinari, R., Knoeller,
989 K., 2015. The Po river water from the Alps to the Adriatic Sea (Italy): new insights from
990 geochemical and isotopic ($\delta^{18}\text{O}$ - δD) data. *Environmental Science and Pollution Research* 22,
991 5184-5203. <http://dx.doi.org/10.1007/s11356-014-3750-6>

992 Martin, C., Bentaleb, I., Kaandorp, R., Iacumin, P., Chatri, K., 2008. Intra-tooth study of

993 modern rhinoceros enamel $\delta^{18}\text{O}$: Is the difference between phosphate and carbonate $\delta^{18}\text{O}$ a
994 sound diagenetic test? *Palaeogeogr. Palaeoclimatol. Palaeoecol.* *Palaeogeogr. Palaeoclimatol.*
995 *Palaeoecol.* 266, 183-189. <http://dx.doi.org/10.1016/j.palaeo.2008.03.039>
996 Martinelli, L.A., Devol, A.H., Victoria, R.L., Richey, J.E., 1991. Stable carbon isotope
997 variation in C3 and C4 plants along the Amazon River. *Nature* 353, 57-59
998 Martinetto, E., 2015. Monographing the Pliocene and Early Pleistocene carpofloras of
999 Italy: methodological challenges and current progress. *Palaeontographica Abt. B.* 293,
1000 57-99.
1001 Martinetto, E., Momohara, A., Bizzarri, R., Baldanza, A., Delfino, M., Esu, D., Sardella, R.,
1002 2015. Late persistence and deterministic extinction of humid thermophilous plant taxa of East
1003 Asian affinity (HUTEA) in southern Europe. *Palaeogeogr. Palaeoclimatol. Palaeoecol.* Online
1004 version, <http://dx.doi.org/10.1016/j.palaeo.2015.08.015>
1005 Masini, F., Ficarelli, G., Torre, D., 1994. Late Villafranchian and the earliest Galerian
1006 mammal Faunas from some intermontane basins of north-central Italy. *Memorie della*
1007 *Societa` Geologica Italiana* 48, 381–389.
1008 Mazza, P., 1988. The Tuscan Early Pleistocene rhinoceros *Dicerorhinus etruscus*.
1009 *Palaeontogr. Ital.* 75, 1-87.
1010 Maxia, C., 1949. Resti di mammiferi rinvenuti nella miniera di lignite di Caste1 S. Pietro
1011 (Sabina). *La Ricerca Scientifica* 19, 346-347.
1012 Metcalfe, J.Z., Longstaffe, F.J., 2012. Mammoth tooth enamel growth rates inferred from
1013 stable isotope analysis and histology. *Quat. Res.* 77, 424-432.
1014 <http://dx.doi.org/10.1016/j.yqres.2012.02.002>
1015 Metcalfe, J.Z., Longstaffe, F.J., Jass, C.N., Zazula, G.D., Keddie, G., 2016. Taxonomy,
1016 location of origin and health status of proboscideans from Western Canada investigated using
1017 stable isotope analysis. *J. Quat. Sci.* 31, 126-142. <http://dx.doi.org/10.1002/jqs.2849>

1018 Metcalfe, J.Z., Longstaffe, F.J., White CD. 2009. Method-dependent variations in stable
1019 isotope results for structural carbonate in bone bioapatite. *J. Archaeol. Sci.* 36, 110-121.
1020 <http://dx.doi.org/10.1016/j.jas.2008.07.019>

1021 Metcalfe, J.Z., Longstaffe, F.J., Zazula, G.D., 2010. Nursing, weaning, and tooth development
1022 in woolly mammoths from Old Crow, Yukon, Canada: Implications for Pleistocene
1023 extinctions. *Palaeogeogr. Palaeoclimatol. Palaeoecol.* 298, 257-270.
1024 <http://dx.doi.org/10.1016/j.palaeo.2010.09.032>

1025 Meyers, S.R., Hinnov, L.A., 2010. Northern Hemisphere glaciation and the evolution of Plio-
1026 Pleistocene climate noise. *Paleoceanography* 25, PA3207.
1027 <http://dx.doi.org/10.1029/2009pa001834>

1028 Mishra, S., Tripathi, A., Tripathi, D.K., Chauhan, D.K., 2015. Role of sedges (Cyperaceae) in
1029 wetlands, environmental cleaning and as food material: Possibilities and future perspectives,
1030 in: Azooz, M.M., Ahmad, P. (Eds.), *Plant-Environment Interaction: Responses and*
1031 *Approaches to Mitigate Stress*. John Wiley & Sons Ltd., Chichester, pp. 327–338.
1032 <http://dx.doi.org/10.1002/9781119081005.ch18>

1033 Montanari, S., Louys, J., Price, G.J., 2013. Pliocene Paleoenvironments of Southeastern
1034 Queensland, Australia Inferred from Stable Isotopes of Marsupial Tooth Enamel. *Plos One* 8,
1035 e66221. <http://dx.doi.org/10.1371/journal.pone.0066221>

1036 O'Leary, M.H., 1988. Carbon Isotopes in Photosynthesis. *BioScience* 38, 328-336.
1037 <http://dx.doi.org/10.2307/1310735>

1038 Palombo, M.R., 2007. What is the boundary for the Quaternary period and Pleistocene epoch?
1039 The contribution of turnover patterns in large mammalian complexes from north-western
1040 Mediterranean to the debate. *Quaternaire* 18, 35-53

1041 Pandolfi, L., 2013. New and revised occurrences of *Dihoplus megarhinus* (Mammalia,
1042 Rhinocerotidae) in the Pliocene of Italy. *Swiss J. Palaeontol.* 132, 239-255.

1043 <http://dx.doi.org/10.1007/s13358-013-0056-0>.

1044 Pandolfi L, Petronio C. 2011. *Stephanorhinus etruscus* (Falconer, 1868) from Pirro Nord
1045 (Apricena, Foggia, Southern Italy) with notes on the other late Early Pleistocene rhinoceros
1046 remains of Italy. Riv. Ital. Paleontol. S. 117, 173-187.

1047 Pandolfi, L., Petronio, C., 2015. Brief note on the occurrences of continental *Hippopotamus*
1048 (Mammalia, Hippopotamidae) in Italy. Geol. Croat. 68, 313-319.
1049 <http://dx.doi.org/104154/gc.2015.24>.

1050 Pandolfi, L., Grossi, F., Frezza, V., 2015. New insights into the Pleistocene deposits of Monte
1051 delle Piche, Rome, and remarks on the biochronology of continental *Hippopotamus*
1052 (Mammalia, Hippopotamidae) and *Stephanorhinus etruscus* (Mammalia, Rhinocerotidae) in
1053 Italy. Estud. Geol. 71, e026. <http://dx.doi.org/10.3989/egeol.41796.337>.

1054 Passey, B.H., Robinson, T.F., Ayliffe, L.K., Cerling, T.E., Sponheimer, M., Dearing, M.D.,
1055 Roeder, B.L., Ehleringer, J.R., 2005. Carbon isotope fractionation between diet, breath CO₂,
1056 and bioapatite in different mammals. J. Archaeol. Sci. 32, 1459-1470.
1057 <http://dx.doi.org/10.1016/j.jas.2005.03.015>

1058 Pellegrini, M., Lee-Thorp, J.A., Donahue, R.E., 2011. Exploring the variation of the delta O-
1059 18(p) and delta O-18(c) relationship in enamel increments. Palaeogeogr. Palaeoclimatol.
1060 Palaeoecol. 310, 71-83. [10.1016/j.palaeo.2011.02.023](http://dx.doi.org/10.1016/j.palaeo.2011.02.023)

1061 Pellegrini, M., Snoeck, C., 2016. Comparing bioapatite carbonate pre-treatments for isotopic
1062 measurements: Part 2 — Impact on carbon and oxygen isotope compositions. Chem. Geol.
1063 420, 88-96. <http://dx.doi.org/10.1016/j.chemgeo.2015.10.038>

1064 Petronio, C., Bellucci, L., Martinetto, E., Pandolfi, L., Salari, L., 2011. Biochronology and
1065 palaeoenvironmental changes from the Middle Pliocene to the Late Pleistocene in Central
1066 Italy. Geodiversitas 33, 485-517. <http://dx.doi.org/10.5252/g2011n3a4>

1067 Pontini, M.R., Bertini, A., 2000. Late Pliocene vegetation and climate in Central Italy: high-

1068 resolution pollen analysis from the Fosso Bianco succession (Tiberino Basin). *Geobios* 33,
1069 519-526. [http://dx.doi.org/10.1016/s0016-6995\(00\)80024-8](http://dx.doi.org/10.1016/s0016-6995(00)80024-8)

1070 Pryor, A.J.E., Stevens, R.E., O'Connell, T.C., Lister, J.R., 2014. Quantification and
1071 propagation of errors when converting vertebrate biomineral oxygen isotope data to
1072 temperature for palaeoclimate reconstruction. *Palaeogeogr. Palaeoclimatol. Palaeoecol.* 412,
1073 99-107. <http://dx.doi.org/10.1016/j.palaeo.2014.07.003>

1074 Pushkina, D., Bocherens, H., Ziegler, R., 2014. Unexpected palaeoecological features of the
1075 Middle and Late Pleistocene large herbivores in southwestern Germany revealed by stable
1076 isotopic abundances in tooth enamel. *Quat. Int.* 339, 164-178.
1077 <http://dx.doi.org/10.1016/j.quaint.2013.12.033>

1078 Quade, J., Cerling, T.E., Barry, J.C., Morgan, M.E., Pilbeam, D.R., Chivas, A.R., Leethorp,
1079 J.A., Vandermerwe, N.J., 1992. A 16-Ma record of paleodiet using carbon and oxygen
1080 isotopes in fossil teeth from Pakistan. *Chem. Geol.* 94, 183-192.
1081 [http://dx.doi.org/10.1016/0168-9622\(92\)90011-x](http://dx.doi.org/10.1016/0168-9622(92)90011-x)

1082 Ravazzi, C., Pini, R., Breda, M., 2009. Reconstructing the palaeoenvironments of the early
1083 Pleistocene mammal faunas from the pollen preserved on fossil bones. *Quat. Sci. Rev.* 28,
1084 2940-2954. <http://dx.doi.org/10.1016/j.quascirev.2009.07.022>

1085 Rivals, F., Mol, D., Lacomat, F., Lister, A.M., Semprebon, G.M., 2015. Resource
1086 partitioning and niche separation between mammoths (*Mammuthus rumanus* and *Mammuthus*
1087 *meridionalis*) and gomphotheres (*Anancus arvernensis*) in the Early Pleistocene of Europe.
1088 *Quat. Int.* 379, 164-170. <http://dx.doi.org/10.1016/j.quaint.2014.12.031>

1089 Rook, L., Martinez-Navarro, B., 2010. Villafranchian: The long story of a Plio-Pleistocene
1090 European large mammal biochronologic unit. *Quat. Int.* 219, 134-144.
1091 <http://dx.doi.org/10.1016/j.quaint.2010.01.007>

1092 Rook, L., Croitor, R., Delfino, M., Ferretti, M., Gallai, G., Pavia, M., 2013. The Upper

1093 Valdarno Plio-Pleistocene vertebrate record: An historical overview, with notes on
1094 palaeobiology and stratigraphic significance of some important taxa. *Ital. J. Geosci.* 132, 104-
1095 125. <http://dx.doi.org/10.3301/IJG.2012.16>

1096 Rozanski, K., Araguás-Araguás, L., Gonfiantini, R., 1993. Isotopic Patterns in Modern Global
1097 Precipitation, in: Swart, P.K., Lohmann, K.C., Mckenzie, J., Savin, S. (Eds.), *Climate Change*
1098 *in Continental Isotopic Records*. American Geophysical Union, Washington, DC., pp.1–36.

1099 Russo Ermolli, E., Sardella, R., Di Maio, G., Petronio, C., Santangelo, N., 2010. Pollen and
1100 mammals from the late Early Pleistocene site of Saticula (Sant'Agata de' Goti, Benevento,
1101 Italy). *Quat. Int.* 225, 128-137. <http://dx.doi.org/10.1016/j.quaint.2009.06.013>

1102 Sacco, F., 1895. Le Rhinocéros de Dusino (*Rhinoceros etruscus* var. *astensis* Sacco).
1103 *Archives du Musée d'Histoire Naturelle de Lyon* 6, 1-31.

1104 Sacco, F. 1906. Resti fossili di Rinoceronti dell'Astigiana. *Memorie della Regia Accademia*
1105 *delle Scienze di Torino*, s. 2 (56), 105–116.

1106 Salzmann, U., Williams, M., Haywood, A.M., Johnson, A.L.A., Kender, S., Zalasiewicz, J.,
1107 2011. Climate and environment of a Pliocene warm world. *Palaeogeogr. Palaeoclimatol.*
1108 *Palaeoecol.* 309, 1-8. DOI: <http://dx.doi.org/10.1016/j.palaeo.2011.05.044>

1109 Scherler, L., Tutken, T., Becker, D., 2014. Carbon and oxygen stable isotope compositions of
1110 late Pleistocene mammal teeth from dolines of Ajoie (Northwestern Switzerland). *Quat. Res.*
1111 82, 378-387. <http://dx.doi.org/10.1016/j.yqres.2014.05.004>

1112 Skrzypek, G., Sadler, R., Wiśniewski, A., 2016. Reassessment of recommendations for
1113 processing mammal phosphate $\delta^{18}\text{O}$ data for paleotemperature reconstruction. *Palaeogeogr.*
1114 *Palaeoclimatol. Palaeoecol.* 446, 162-167. <http://dx.doi.org/10.1016/j.palaeo.2016.01.032>

1115 Spötl, C., Vennemann, T.W., 2003. Continuous-flow isotope ratio mass spectrometric
1116 analysis of carbonate minerals. *Rapid Commun. Mass Spectrom.* 17, 1004-1006.
1117 <http://dx.doi.org/10.1002/rcm.1010>

1118 Sullivan, C.H., Krueger, H.W., 1981. Carbon isotope analysis of separate chemical phases in
1119 modern and fossil bone. *Nature* 292, 333-335. [http://dx.doi.org/ 10.1038/292333a0](http://dx.doi.org/10.1038/292333a0)

1120 Tafforeau, P., Bentaleb, I., Jaeger, J.-J., Martin, C., 2007. Nature of laminations and
1121 mineralization in rhinoceros enamel using histology and X-ray synchrotron
1122 microtomography: Potential implications for palaeoenvironmental isotopic studies.
1123 *Palaeogeogr. Palaeoclimatol. Palaeoecol.* 246, 206-227.
1124 <http://dx.doi.org/10.1016/j.palaeo.2006.10.001>

1125 Teodoridis, V., Bruch, A.A., Vassio, E., Martinetto, E., Kvaček, Z., Stuchlik, L., 2015. Plio-
1126 Pleistocene floras of the Vildštejn Formation in the Cheb Basin, Czech Republic – a floristic
1127 and palaeoenvironmental review. *Palaeogeogr. Palaeoclimatol. Palaeoecol.* Online version,
1128 <http://dx.doi.org/10.1016/j.palaeo.2015.09.038>.

1129 Thorp, J.L., Vandermerwe, N.J., 1987. Carbon isotope analysis of fossil bone apatite. *S. Afr.*
1130 *J. Sci.* 83, 712-715

1131 Tipple, B.J., Meyers, S.R., Pagani, M., 2010. Carbon isotope ratio of Cenozoic CO₂: A
1132 comparative evaluation of available geochemical proxies. *Paleoceanography* 25.
1133 <http://dx.doi.org/10.1029/2009pa001851>

1134 Tütken, T., Furrer, H., Vennemann, T.W., 2007. Stable isotope compositions of mammoth
1135 teeth from Niederweningen, Switzerland: Implications for the Late Pleistocene climate,
1136 environment, and diet. *Quat. Int.* 164-65, 139-150.
1137 <http://dx.doi.org/10.1016/j.quaint.2006.09.004>

1138 Tütken, T., Kaiser, T.M., Vennemann, T., Merceron, G., 2013. Opportunistic Feeding
1139 Strategy for the Earliest Old World Hypsodont Equids: Evidence from Stable Isotope and
1140 Dental Wear Proxies. *Plos One* 8, e74463. <http://dx.doi.org/10.1371/journal.pone.0074463>

1141 Tütken, T., Vennemann, T.W., Janz, H., Heimann, E.P.J., 2006. Palaeoenvironment and
1142 palaeoclimate of the Middle Miocene lake in the Steinheim basin, SW Germany: A

1143 reconstruction from C, O, and Sr isotopes of fossil remains. *Palaeogeogr. Palaeoclimatol.*
1144 *Palaeoecol.* 241, 457-491. <http://dx.doi.org/10.1016/j.palaeo.2006.04.007>

1145 Vennemann, T.W., Fricke, H.C., Blake, R.E., O'Neil, J.R., Colman, A., 2002. Oxygen isotope
1146 analysis of phosphates: a comparison of techniques for analysis of Ag₃PO₄. *Chem. Geol.*
1147 185, 321-336. [http://dx.doi.org/10.1016/s0009-2541\(01\)00413-2](http://dx.doi.org/10.1016/s0009-2541(01)00413-2)

1148 Vialli, V., 1956. Sul rinoceronte e l'elefante dei livelli superiori della serie lacutre di Leffe
1149 (Bergamo). *Memorie della Società Italiana di Scienze Naturali (Museo Civico di Storia*
1150 *Naturale di Milano)*, Milano, 12 (1), 1-71.

1151 Wang, Y., Cerling, T.E., 1994. A model of fossil tooth and bone diagenesis: implications for
1152 paleodiet reconstruction from stable isotopes. *Palaeogeogr. Palaeoclimatol. Palaeoecol.* 107,
1153 281-289. [http://dx.doi.org/10.1016/0031-0182\(94\)90100-7](http://dx.doi.org/10.1016/0031-0182(94)90100-7)

1154 Woodard, S.C., Rosenthal, Y., Miller, K.G., Wright, J.D., Chiu, B.K., Lawrence, K.T., 2014.
1155 Antarctic role in Northern Hemisphere glaciation. *Science* 346, 847-851.
1156 <http://dx.doi.org/10.1126/science.1255586>

1157 Zanazzi, A., Judd, E., Fletcher, A., Bryant, H., Kohn, M.J., 2015. Eocene-Oligocene
1158 latitudinal climate gradients in North America inferred from stable isotope ratios in
1159 perissodactyl tooth enamel. *Palaeogeogr. Palaeoclimatol. Palaeoecol.* 417, 561-568.
1160 <http://dx.doi.org/10.1016/j.palaeo.2014.10.024>

1161 Zazzo, A., Lecuyer, C., Mariotti, A., 2004a. Experimentally-controlled carbon and oxygen
1162 isotope exchange between bioapatites and water under inorganic and microbially-mediated
1163 conditions. *Geochim. Cosmochim. Acta* 68, 1-12. [http://dx.doi.org/10.1016/s0016-](http://dx.doi.org/10.1016/s0016-7037(03)00278-3)
1164 [7037\(03\)00278-3](http://dx.doi.org/10.1016/s0016-7037(03)00278-3)

1165 Zazzo, A., Lecuyer, C., Sheppard, S.M.F., Grandjean, P., Mariotti, A., 2004b. Diagenesis and
1166 the reconstruction of paleoenvironments: A method to restore original delta O-18 values of

1167 carbonate and phosphate from fossil tooth enamel. *Geochim. Cosmochim. Acta* 68, 2245-
1168 2258. <http://dx.doi.org/10.1016/j.gca.2003.11.009>

1169

1170

1171 **Figures and table captions**

1172

1173 **Figure 1.** Location of paleontological sites cited in Table A1 (the map shows the present day
1174 locations.)

1175

1176 **Figure 2.** Average $\delta^{13}\text{C}$ (‰, VPDB) and $\delta^{18}\text{O}_{\text{PO}_4}$ (‰, VSMOW) values obtained from the
1177 teeth with calculated environmental water values, relative MAT scales and vegetation
1178 estimation. A) North Italy B) Central Italy,

1179 Vegetation information is from Domingo et al. (2013), environmental water values were
1180 calculated by applying Equation 3. (after Kohn and Cerling, 2002), relative MAT scales were
1181 calculated using the minimum and maximum slopes of the equations from Table 2.

1182 Chronology according to Hilgen et al (2012). The onset of the Quaternary according to the
1183 chronology confirmed in 2009 by the International Union of Geological Sciences. NHG =
1184 Northern Hemisphere Glaciation, MPWP = “Mid-Pliocene Warm Period”, VMT =
1185 Villafranchian mammal turnover, EEQ = Elephant-Equus event, the * sign represent an
1186 outlier in Central Italy in MNQ19.

1187

1188 **Table 1.** Calculated MAT changes based on $\delta^{18}\text{O}_{\text{PO}_4}$ and vegetation estimates based on the
1189 $\delta^{13}\text{C}_{\text{CO}_3}$ isotope results compared with palaeobotanical proxies, (1) Bertini, 2001; (2) Bertini,
1190 2010; (3) Fauquette et al., 1999; (4) Combourieu-Nebout et al., 2015; (5) Fauquette and
1191 Bertini, 2003; (6) Magri et al., 2009; (7) Klotz et al., 2006; (8) Fauquette et al., 2006; MLV:
1192 most likely value, NHG: Northern Hemisphere Glaciation.

1193

1194 **Table 2.** The equations used for the calculations of water $\delta^{18}\text{O}$ values from those measured for
1195 the phosphates.

1196

1197 **Appendix**

1198 **Table A1.** Locations and age estimates for the fossil localities, measured carbon and oxygen
1199 isotopic compositions, calculated isotopic composition of diet and environmental water.
1200 Selected references give information about the palaeontology and the geological settings of
1201 the fossils. Institutional abbreviations are explained in the text.

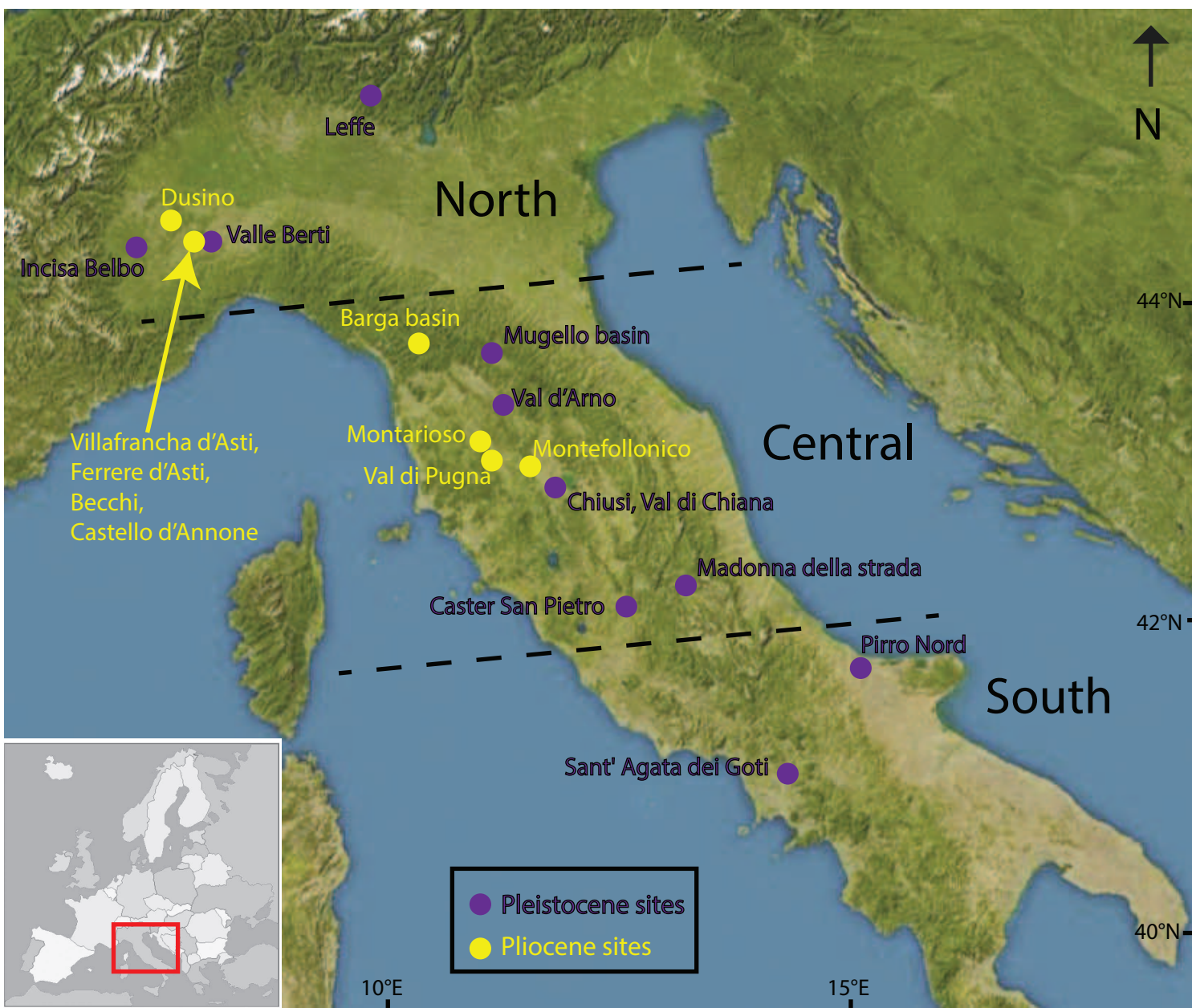
Table

	age (Ma)	~5.2 - 3.5	~3.3 - 2.8	~2.8-2.5	~2.5-1.9	~1.9-1.7	~1.7-1.3	~1.3-1	recent
	MN zone	MN14-15	MN16a	MN16b	MN17	MNQ18	MNQ19	MNQ19-20	
Central Italy	MAT changes (°C) indications (this study)		2 - 3.6 °C decrease of MAT from MN14			2 - 3.6 °C decrease of MAT from MNQ18 to MNQ19-20			
	estimated vegetation (this study)	woodland-mesic grassland	woodland-mesic grassland			woodland-mesic grassland, more open vegetation / less humid / less precipitation than in the former biozones	woodland-mesic grassland	woodland-mesic grassland, more open vegetation / less humid / less precipitation than in the former biozones	
	palaeobotanical indications			open vegetation at 2.7, NHG (1)	Interglacials: higher MAT and MAP than present day. Glacials: similar MAT and MAP to present day (2), vegetation openings at 2.5Ma and from 1.9 to 1.7Ma (MNQ18) (1)				MAT 14-16 °C, MAP 760-970mm (4), 730mm (6)
North Italy	estimated vegetation (this study)	woodland-mesic grassland	woodland-mesic grassland	woodland-mesic grassland, more open vegetation / less humid / less precipitation than in MN6a		woodland-mesic grassland, (one sample from Leffe indicate open woodland-xeric grassland)			
	palaeobotanical indications	MAT 16-20 °C (MLV 17-19°C) (1;2), 12-20 °C (3), 1-4 °C higher than present day (8), 1100-1600mm (MLV 1200-1300mm) (1,2), 1100-1400mm (3), 400-700mm higher than present day (8)			Interglacials: similar MAP and MAT to Early Pliocene, Glacials: similar MAT to present day, and 500-600mm higher MAP than present, (5) (Stirone site), alternations of different types of forests with no open vegetation (2)				MAT, 13-15 °C, MAP 930-1100mm (4)
South Italy	estimated						woodland-mesic grassland		
	palaeobotanical indications	>22 °C, equal to or 5 °C higher than present day (8), 600mm (3), drier or equal humidity than present day (8), some subdesertic plants (2)			Interglacials: MAT 2.8 °C higher than today, MAP 500mm higher than today, Glacials: MAT lower than today, MAP equal to present day, (7) (Semaforo site)			open vegetation and forest alternations (2)	MAT, 15-18 °C, MAP 440-830mm (4)

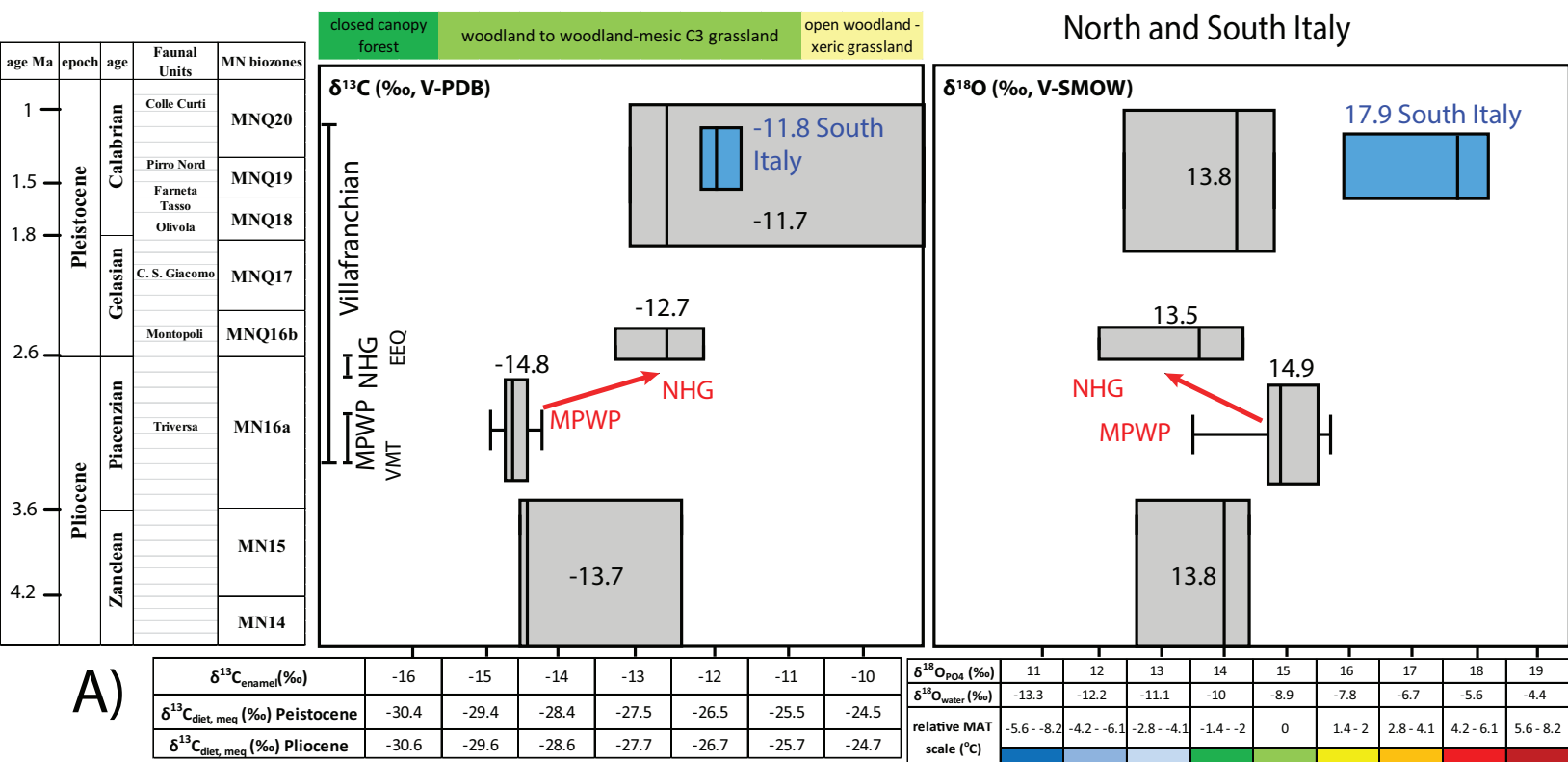
Table

Number of equation	Relationship	Equation	type of regression	R ² , slope	References
1	$\delta^{13}C_{\text{diet, meq}}; \delta^{13}C_{\text{leaf}}$	$\delta^{13}C_{\text{diet, meq}} = \delta^{13}C_{\text{leaf}} + (\delta^{13}C_{\text{modernatmCO2}} - \delta^{13}C_{\text{ancientatmCO2}})$			Domingo et al., (2013)
2	$\delta^{13}C_{\text{diet, meq}}; MA_p$	$\delta^{13}C_{\text{diet, meq}}(\text{‰}, \text{VPDB}) = -10.29 + 1.9 \times 10^{-4} \text{ altitude (m)} - 5.61 \log_{10}(\text{MAP} + 300, \text{ mm/yr}) - 0.0124 \text{ Abs (latitude, } \circ)$			Kohn, (2010)
3	$\delta^{18}O_w; \delta^{18}O_{PO4}$	$\delta^{18}O_w = (\delta^{18}O_{PO4} - 23) / 0.90$	inverted forward regression	slope = 1.11	Kohn and Cerling, (2002)
4	$\delta^{18}O_w; \delta^{18}O_{PO4}$	$\delta^{18}O_w = (\delta^{18}O_{PO4} - 26.8 + 8.9h) / 0.76$; (where h is the relative humidity)	inverted forward regression	slope = 1.32	Kohn, (1996)
5	$\delta^{18}O_w; \delta^{18}O_{PO4}$	$\delta^{18}O_w = 1.1128 (\pm 0,0029) \delta^{18}O_{PO4} - 26.4414 (\pm 0.0508)$	transposed regression	R ² = 0.998; slope = 1.11	Amiot et al., (2004)
6	$\delta^{18}O_w; \delta^{18}O_{PO4}$	$\delta^{18}O_w = (\delta^{18}O_{PO4} - 23.3 (\pm 0.7)) / 0.94 (\pm 0.10)$	inverted forward regression	R ² = 0.85; slope = 1.06	Ayliffe et al., (1992)
7	MAT; $\delta^{18}O_w$; for Europe	$MAT = (\delta^{18}O_w + 13.74) / 0.53$	inverted forward regression	R ² = 0.6, slope = 1.89	Pryor et al., (2014)
8	MAT; $\delta^{18}O_w$; for Europe	$MAT = 1.41 \delta^{18}O_w + 21.64$	transposed regression	R ² = 0.49, slope = 1.41	Skrzypek et al., (2016)
9	MAT; $\delta^{18}O_w$; for Italy (excluded the islands)	$MAT = 1.56 \delta^{18}O_w + 23.31$	transposed regression	R ² = 0.3, slope = 1.56	data of GNIP stations from Skrzypek et al., (2016)
10	MAT; $\delta^{18}O_w$; global equation	$MAT = (\delta^{18}O_w + 13.6) / 0.69$	inverted forward regression	slope = 1.45	Dansgaard, (1964)
11	MAT; $\delta^{18}O_w$; global equation	$MAT = (\delta^{18}O_w + 14.18 \pm 0.52) / (0.49 \pm 0.03)$	inverted forward regression	R ² = 0.81; slope = 2.04	Amiot et al., (2004)

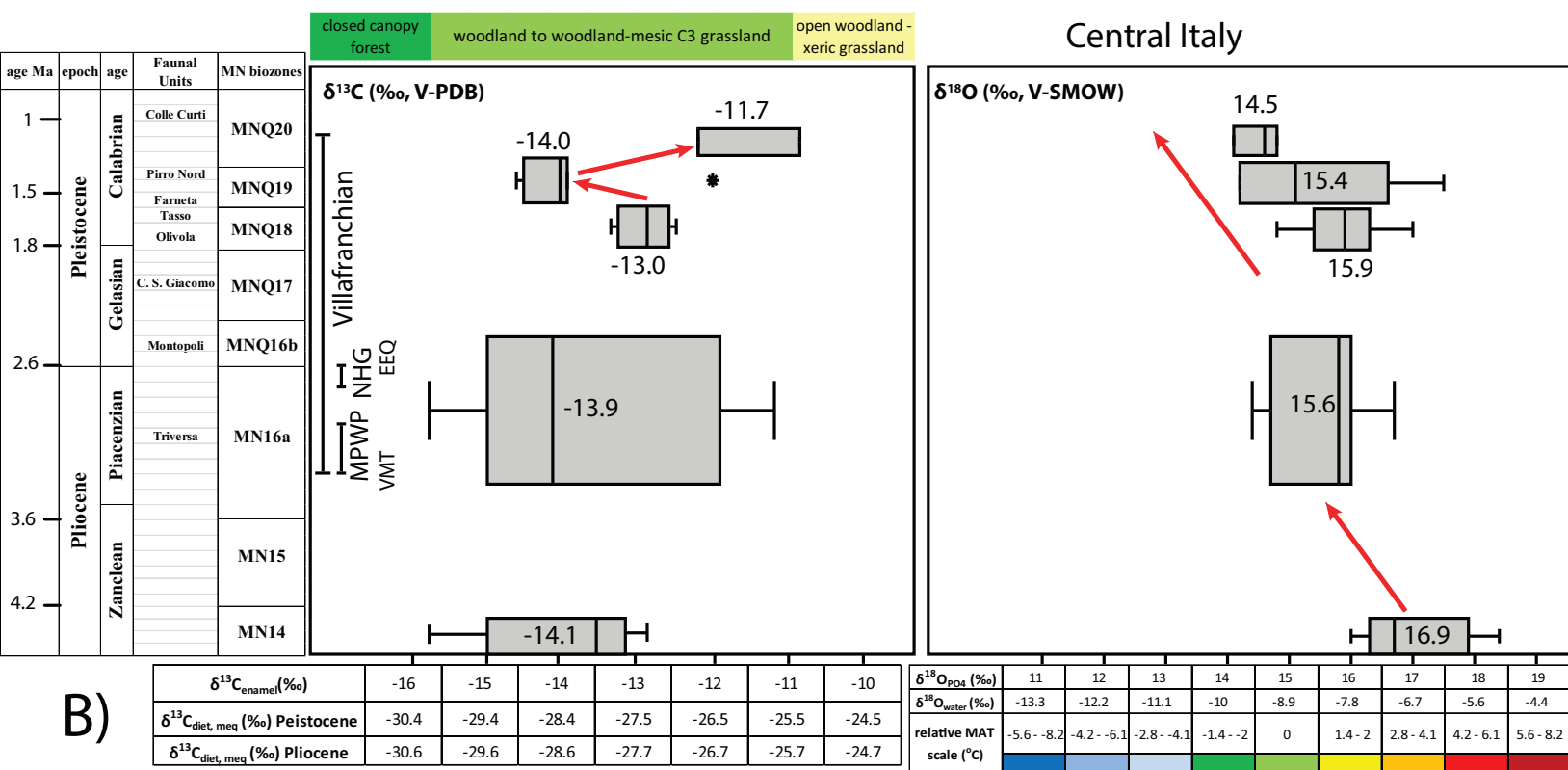
Figure



Figure



A)



B)

Highlights

- $\delta^{13}\text{C}_{\text{CO}_3}$ results indicate that the investigated taxa were grazers-browsers in a pure C_3 vegetation.
- According to the $\delta^{18}\text{O}_{\text{PO}_4}$ results Pliocene was characterized by higher temperatures than Early Pleistocene in Central Italy
- In North Italy the $\delta^{13}\text{C}$ values show a sharp increase between MN16a and MNQ16b biozones that is most likely linked to the Northern Hemisphere Glaciation at 2.7 Ma.
- Higher $\delta^{13}\text{C}$ values in MNQ18 and MNQ19-20 biozones in Central Italy are in agreement with pollen data indicating more open vegetation than in the Pliocene.

Supplementary Data

[Click here to download Supplementary Data: table_A1.xlsx](#)